

Journal of the Geological Society

Petrology, Sr Nd Hf isotopic geochemistry and zircon chronology of the Late Palaeozoic volcanic rocks in the southwestern Tianshan Mountains, Xinjiang, NW China

YONGFENG ZHU, XUAN GUO, BIAO SONG, LIFEI ZHANG and LIBING GU

Journal of the Geological Society 2009; v. 166; p. 1085-1099
doi:10.1144/0016-76492008-130

Email alerting service

[click here](#) to receive free email alerts when new articles cite this article

Permission request

[click here](#) to seek permission to re-use all or part of this article

Subscribe

[click here](#) to subscribe to Journal of the Geological Society or the Lyell Collection

Notes

Downloaded by on 28 October 2009

Petrology, Sr–Nd–Hf isotopic geochemistry and zircon chronology of the Late Palaeozoic volcanic rocks in the southwestern Tianshan Mountains, Xinjiang, NW China

YONGFENG ZHU^{1*}, XUAN GUO¹, BIAO SONG², LIFEI ZHANG¹ & LIBING GU¹

¹*The Key Laboratory of Orogenic Belts and Crustal Evolution, School of Earth and Space Sciences, Peking University, Beijing 100871, China*

²*Beijing SHRIMP Center, Chinese Academy of Geological Sciences, Beijing 100037, China*

**Corresponding author (e-mail: yfzhu@pku.edu.cn)*

Abstract: The Late Palaeozoic volcanic rocks, mainly consisting of basalt, trachyte, trachy-andesite, andesite and rhyolite, widely distributed in the southwestern Tianshan Mountains, have been proven to be formed during Late Devonian to Late Carboniferous time (>361–313 Ma) based on zircon sensitive high-resolution ion microprobe dating. The geochemistry demonstrates that the studied volcanic rocks represent a continental arc formed during the subduction of the Palaeo-southern Tianshan Ocean. The $\epsilon_{\text{Hf}(T)}$ values of zircons in these volcanic rocks vary from +1.4 to +15.6 with weighted average values of +9.5 (Late Devonian), +8.9 (Early Carboniferous) and +10.3 (Late Carboniferous), suggesting a depleted mantle origin. However, the Late Devonian basaltic samples have negative $\epsilon_{\text{Nd}(T)}$ values (from –5.16 to –3.07) and high initial $^{87}\text{Sr}/^{86}\text{Sr}$ ratios (0.7073–0.7098), whereas the Early Carboniferous volcanic rocks mostly have positive $\epsilon_{\text{Nd}(T)}$ values (from –0.18 to +3.07) with low initial $^{87}\text{Sr}/^{86}\text{Sr}$ ratios (0.7044–0.7067), and the Late Carboniferous volcanic rocks are characterized by high $\epsilon_{\text{Nd}(T)}$ values (+2.79 to +5.89) and low initial $^{87}\text{Sr}/^{86}\text{Sr}$ ratios (0.7032–0.7054). The assimilation–fractional crystallization (AFC) model is used to explain the isotope characteristics of the Late Devonian volcanic rocks in the southwestern Tianshan Mountains. Calculation shows that the Late Devonian samples could be formed by the AFC process between depleted mantle and continental crust. The Carboniferous basaltic rocks originated by partial melting of the mantle wedge.

Supplementary material: Data are available at <http://www.geolsoc.org.uk/SUP18378>.

The evolution of the Palaeo-southern Tianshan Ocean (one of the major constituents of the Palaeo-Central Asian Ocean) has been hotly debated in the recent literature. The key issue is the time of closing of the Palaeo-southern Tianshan Ocean and the nature of its related continental arc system. Occurrences of ophiolite, blueschist and eclogites were reported along the major fault (i.e. Nikulaev line, see Fig. 1a and b) of the southwestern Tianshan Mountains, and studies on these rocks provided controversial conclusions. Some researchers suggested that the Palaeo-southern Tianshan Ocean closed by the end of the Early Palaeozoic (Shi *et al.* 1994), whereas others believed that it closed during the Late Palaeozoic (Windley *et al.* 1990; Gao *et al.* 1998; Chen *et al.* 1999; Maksumova *et al.* 2001; Xiao *et al.* 2006). Zhang *et al.* (2007) suggested that the Palaeo-southern Tianshan Ocean probably did not close until the Triassic period, based on zircon chronology studies of retrograded coesite eclogites from the southwestern Tianshan Mountains. In most cases, Late Palaeozoic volcano-sedimentary strata cover Proterozoic to Silurian sedimentary–metamorphic rocks in the southwestern Tianshan Mountains. These Late Palaeozoic volcano-sedimentary rocks, widely exposed in the southwestern Tianshan Mountains, consist of rhyolite, trachyte, trachy-andesite, basalt, tuff with volcanic clastic sedimentary rocks, sandstone and limestone (Qian *et al.* 2006; Zhu *et al.* 2006a). Early studies suggested that these volcanic rocks are related to rifting (Che *et al.* 1996) or to a large igneous province associated with a mantle plume (Xia *et al.* 2004). However, the mantle plume

hypothesis could not be proven, as the Late Palaeozoic volcanic rocks in the southwestern Tianshan Mountains consist mainly of felsic volcanic rocks (>70 vol.%, andesite, rhyolite, tuff and clastic sedimentary rocks) with less significant amounts of basaltic rocks. Basaltic rocks are absent in some regions (especially in the eastern part of the southwestern Tianshan Mountains; see Zhu *et al.* 2005). Recent studies suggested that these volcanic rocks were formed in a continental arc environment (Zhu *et al.* 2005, 2006a; Qian *et al.* 2006; Zhao *et al.* 2007; Wang, B., *et al.* 2007). We believe that the ‘plume hypothesis’ cannot be applied to the southwestern Tianshan Mountains for the following reasons: (1) the typical rock associations of a large igneous province are absent; (2) the exposure area of the volcanic rocks is much smaller than that of the Emeishan basalts (Xu *et al.* 2001) and the Columbia River basalts (Coffin & Eldholm 1994; the Columbia River basalts probably represent the smallest large igneous province reported in the geological literature). In this study, we show that the age range of these volcanic rocks is greater than 50 Ma, which is inconsistent with one large igneous province erupted in a short period. Providing a correct interpretation of the genesis of these volcanic rocks is important for understanding the tectonic evolution of the southwestern Tianshan Mountains. Here we present detailed data on petrology, element geochemistry, Sr–Nd–Hf isotopic geochemistry and zircon chronology to constrain the genesis of the Late Palaeozoic volcanic rocks in the southwestern Tianshan Mountains.

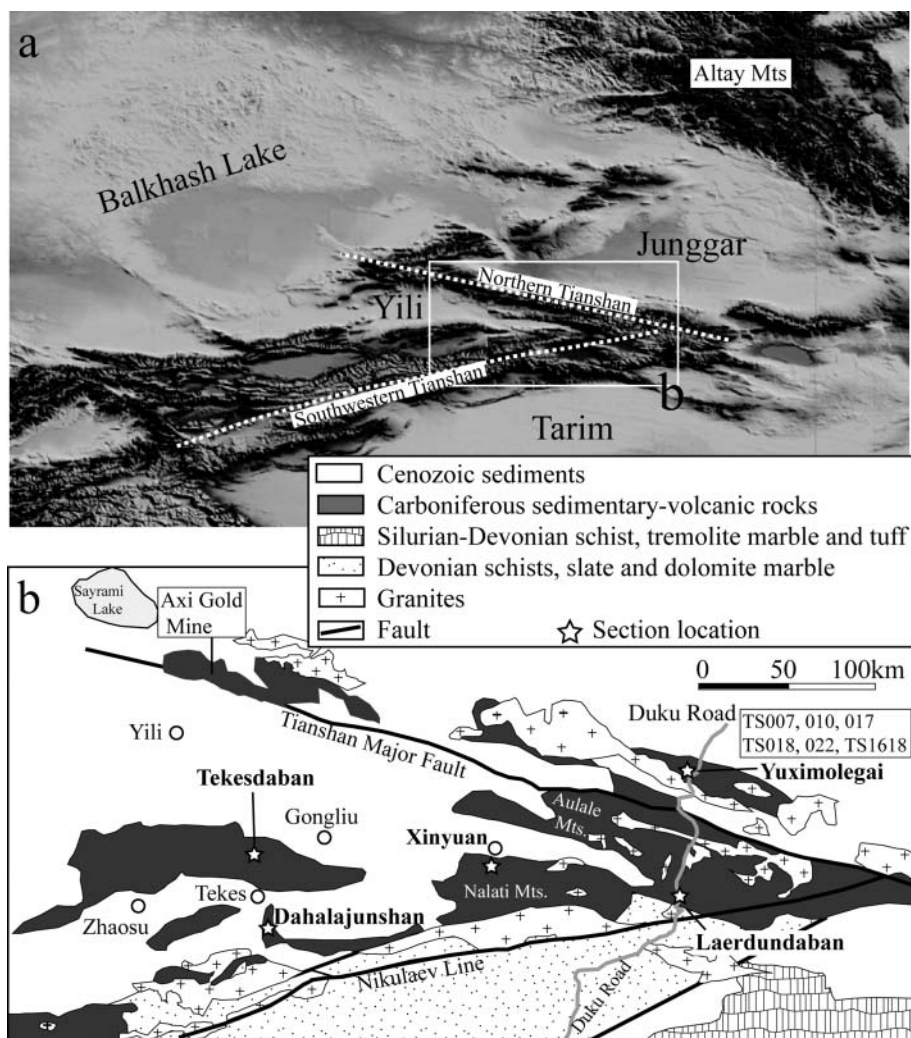


Fig. 1. (a) Digital elevation matrix image of Central Asia showing, from north to south, the Altay Mountains, the Junggar basin, the Tianshan Mountains and the Tarim basin; (b) tectonic-geological sketch map of the southwestern Tianshan Mountains (modified from Zhu *et al.* 2006a). Locations of samples collected in Yuximolegai (the eastern part of the southwestern Tianshan Mountains) are shown.

Regional geology

The triangular-shaped Yili terrane (referred to as central Tianshan) is sandwiched within the north Tianshan and southwestern Tianshan orogenic belts and widens westwards into Kazakhstan and Kyrgyzstan (Fig. 1a). The Tianshan major fault divides the Yili terrane from its northern orogenic belt (i.e. north Tianshan). The Nikulaev line serves as the boundary between the Yili terrane and the southwestern Tianshan orogenic belt (Fig. 1b). The Proterozoic to Silurian sedimentary-metamorphic rocks are overlain by distinctly different Late Palaeozoic volcano-sedimentary strata (Wang *et al.* 1994). In the Vendian-Early Cambrian, sedimentary continental shelf and slope sequences were deposited. Silurian neritic clastic sedimentary rocks, carbonates and interlayered intermediate-acid volcanic rocks and Devonian-Carboniferous mafic-intermediate volcanites crop out in the northern and southern parts of the Yili terrane. The Upper Devonian to Lower Carboniferous sequence is a c. 1000 to >10000 m thick series of limestone, sandstone and shale with volcanic rocks, and the Upper Carboniferous sequence consists of limestone intercalated with volcano-clastic sandstone and medium to acid volcanic rocks with felsic tuff and clastic sedimentary rocks. The overlying Permian strata are made up of continental clastic sedimentary rocks and post-collisional volcanic rocks.

This paper focuses on the Late Palaeozoic volcanic rocks distributed on the southern edge of the Yili terrane. Four sections of Late Palaeozoic volcano-sedimentary rocks in the southwestern Tianshan Mountains have been studied here. From west to east these sections are Tekesdaban (Fig. 2a), Dahalajunshan (Fig. 2b), Xinyuan (Fig. 2c) and Laerdundaban-Yuximolegai (Figs 1b and 2d). Late Palaeozoic basaltic rocks occur mostly in the western region (Tekesdaban and Dahalajunshan) although these rocks occupy less than 30% of the volume of the volcano-sedimentary section. In the western part of the southwestern Tianshan Mountains (i.e. Tekes-Zhaosu-Gongliu), volcanic rocks consist mainly of basalt, basaltic andesite, andesite, rhyolite with tuff and volcanic clastic sedimentary rocks, covering Silurian strata with angular discontinuity (or faulting contact, Figs 1b and 2a,b). The eclogite-bearing blueschist is overlain by these volcanic rocks in the southern Zhaosu region. Sandstone, silt, tuff with clastic sedimentary rocks, and slate are covered by volcanic rocks, mainly consisting of basaltic andesite, andesite and trachy-andesite in the Tekesdaban region (from Gongliu to Tekes town, Fig. 2a). Sample TS08 of fresh basaltic andesite in the middle of this section was collected for zircon separation. The Dahalajunshan section, located to the south of Tekes town, consists mainly of basalt and andesite with volcanic tuff and clastic sedimentary rocks (Fig. 2b). These

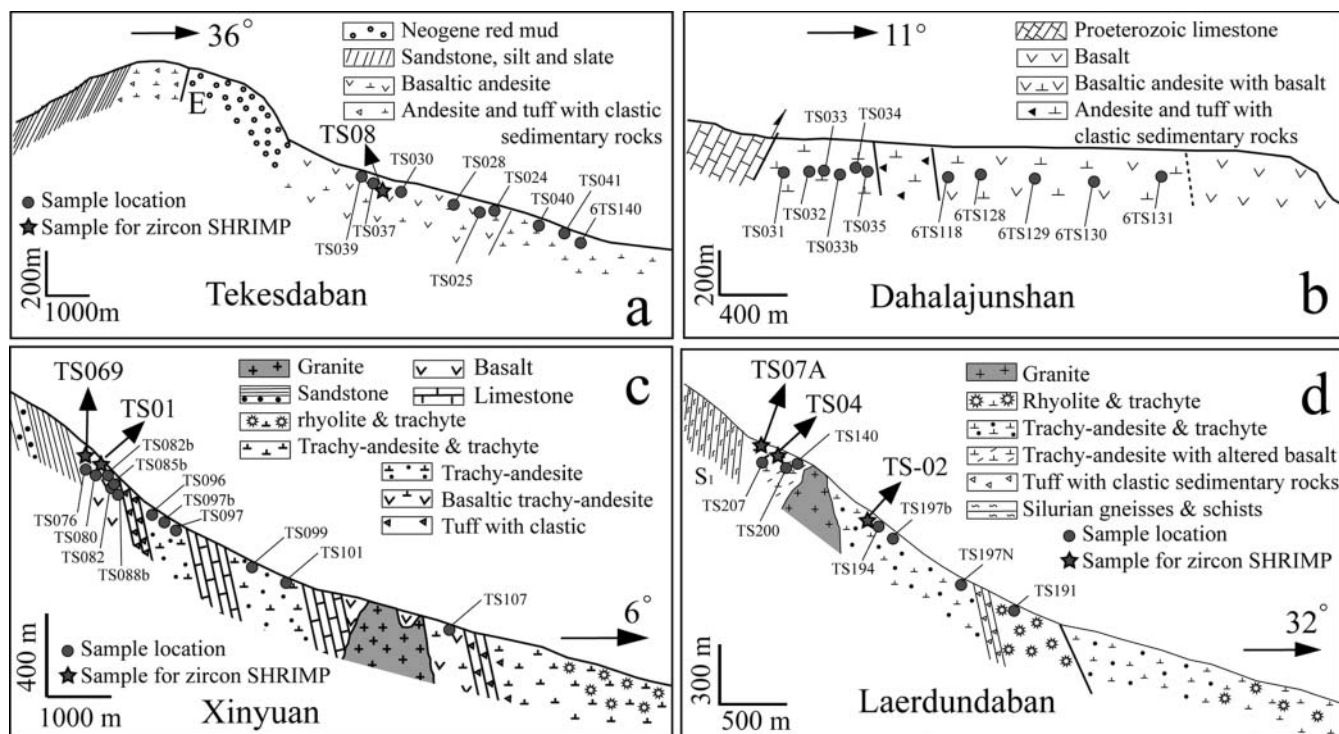


Fig. 2. (a) Geological section for the volcanic rocks in Teksedaban. TS08 is the location of the sample for zircon SHRIMP dating. (b) Geological section for the volcanic rocks in Dahalajunshan. (c) Geological section for the volcanic rocks in Xinyuan. TS01 and TS069 are the sample numbers for zircon SHRIMP dating. (d) Geological section for the volcanic rocks in Laerdundaban. TS02 and TS04 are the sample numbers for zircon SHRIMP dating. Samples for geochemical studies are also shown in these sections.

rocks are in thrust contact with Proterozoic marble and limestone.

Towards the east (in Xinyuan region), andesite to rhyolite with tuff and volcanoclastic sedimentary rocks are the major components (generally >80 vol.%) of the volcano-sedimentary sequences. The Xinyuan section (Fig. 2c) with two limestone interlayers, consists principally of basalt, basaltic andesite interlayered with tuff in the lower part, trachy-andesite and basaltic trachy-andesite with tuff and clastic sedimentary rocks in the middle part, and rhyolite with clastic sedimentary rocks in the upper part. The thickness of volcanic and clastic-carbonate rocks is nearly equal in this section, forming a basin filled with volcanic rocks and oceanic-continental sedimentary rocks.

Further east (the Laerdundaban section), the volcano-sedimentary rocks, directly covering Silurian metamorphic rocks (Fig. 2d), mainly consist of trachy-andesite (with lenses of strongly altered basaltic rocks at the bottom of the sequence) and basaltic trachy-andesite in the lower part, trachyte, rhyolite and tuff in the middle part, and trachy-andesite, trachyte and rhyolite in the upper part. Rhyolite, dacite and andesite, widely occurring in the Yuximolegai region to the north of the Laerdundaban region along the Duku road (see Fig. 1b), were also collected for geochemical study and zircon sensitive high-resolution ion microprobe (SHRIMP) dating. Late Carboniferous gabbros (Zhu *et al.* 2006b; Xue & Zhu 2009) and Permian granites (Wang, C., *et al.* 2007) intruded the Late Palaeozoic volcano-sedimentary units covering the Yili terrane and the southwestern Tianshan Mountains.

Analytical methods

Whole-rock samples were ground in an agate mill, after careful washing in distilled water. Major elements were measured by

X-ray fluorescence (XRF) spectrometry on glass discs made by fusion of whole-rock powder with lithium metaborate. Trace element contents of whole-rock samples were analysed by quadrupole inductively coupled plasma-mass spectrometry (Q-ICP-MS) at the Institute of Geology & Geophysics (IGG), Chinese Academy of Science. Reference materials JP-3, GSR-1 and JSR-3 were used to control the data quality. Results of our calibration analyses compared consistently well with the reference values (e.g. the recommended La, Zr and Sr values for JP3 are 8.81 ppm, 97.8 ppm and 403 ppm (Imai *et al.* 1995), respectively; our measured La, Zr and Sr contents are 8.96–8.84 ppm, 91.84–92.13 ppm and 386.4–394.4 ppm, respectively). This quality control demonstrated that the precision of our analyses is <10% deviation from true values for most trace elements except Cs and Ho relative to JP3. However, relative to GSR1 and GSR3 (Xie *et al.* 1989), the precision of our analyses for all trace elements is <10% deviation from true values.

Samples for isotopic analysis were dissolved in Teflon bombs after being spiked with ^{84}Sr , ^{87}Rb , ^{150}Nd and ^{147}Sm tracers prior to HF + HNO₃ (2:1) dissolution. Strontium and neodymium were extracted by conventional ion exchange chromatographic techniques. Sr and Nd isotope ratios were measured by thermal ionization mass spectrometry (TIMS) using a Finnigan MAT 262 multiple collector system running in dynamic mode at the IGG. Replicate analyses of the Sr isotope reference material BCR-1 gave an average $^{87}\text{Sr}/^{86}\text{Sr}$ value of 0.705086 ± 0.000011 (1σ , $n = 16$; recommended value for BCR-1 is 0.70501 ± 8 , Balcaen *et al.* 2005). The $^{87}\text{Sr}/^{86}\text{Sr}$ ratio was corrected for instrumental mass fractionation assuming $^{86}\text{Sr}/^{88}\text{Sr} = 0.1194$. The $^{143}\text{Nd}/^{144}\text{Nd}$ ratio was corrected for instrumental mass fractionation assuming $^{146}\text{Nd}/^{144}\text{Nd} = 0.7219$. The Nd La Jolla reference material yielded an average ratio of $^{143}\text{Nd}/^{144}\text{Nd} = 0.511842 \pm$

0.000012 (1σ , $n = 12$; recommended value for Nd La Jolla is 0.511849, Upadhyay *et al.* 2008). Blanks were of the order of <0.3 ng for Sr and <0.1 ng for Nd. The Nd isotope data were normalized to the accepted reference values for La Jolla.

Zircon was hand picked under a microscope. Cathodoluminescence (CL) images were obtained for zircons using a CAMECA SX-50 microprobe. Zircons were dated using the SHRIMP II installed at the Beijing SHRIMP Center, and the data correction was based on Williams (1998). *In situ* zircon Hf isotopic analyses were conducted by multi-collector (MC)-ICP-MS using a ThermoFinnigan Neptune system, coupled to a GeoLas 193 nm ArF excimer laser ablation system at the IGG. Spot sizes of 32 μm with a laser repetition rate of 10 Hz at 100 mJ were used during analyses. Raw count rates for ^{172}Yb , ^{173}Yb , ^{175}Lu , $^{176}(\text{Hf} + \text{Yb} + \text{Lu})$, ^{177}Hf , ^{178}Hf , ^{179}Hf , ^{180}Hf and ^{182}W were collected. It is essential that isobaric interference corrections for ^{176}Lu and ^{176}Yb on ^{176}Hf are determined precisely. ^{176}Lu was calibrated using the ^{175}Lu value and the correction was made to ^{176}Hf . The $^{176}\text{Yb}/^{172}\text{Yb}$ value of 0.5887 and mean Yb value obtained during Hf analysis on the same spot were applied for the interference correction of ^{176}Yb on ^{176}Hf (Iizuka & Hirata 2005). The detailed analytical technique has been described by Wu *et al.* (2006). During analyses, the $^{176}\text{Hf}/^{177}\text{Hf}$ ratio of the standard zircon (91500) was 0.282323 ± 25 (2σ , $n = 17$), similar to the commonly accepted $^{176}\text{Hf}/^{177}\text{Hf}$ values of 0.282302 ± 8 and 0.282306 ± 8 (2σ) measured using the solution method (Goolaerts *et al.* 2004; Woodhead *et al.* 2004).

Results

Zircon chronology

Zircons separated from representative rock samples were subjected to chronology studies. The results are shown in Figures 3–7.

Zircons from the Tekesdaban basaltic andesite (TS08)

Zircons with clear magmatic zonation in TS08 are mainly short columnar (Fig. 3a–f). Some zircons have cores. The rims of 18 zircon grains were studied and the results are shown in Fig. 3g–i. The apparent ages of measured zircon rims vary between 342 and 388 Ma. One zircon core has an apparent age of 817 Ma with Th/U ratio of 0.69 (TS08-10.1). The contents of U (76–1277 ppm) and Th (39–1313 ppm) are highly variable and show a linear correlation (Fig. 3j and k). Their $^{232}\text{Th}/^{238}\text{U}$ ratios range between 0.52 and 1.37. The SHRIMP data for all other zircon rims plot on U–Pb concordia and have a weighted average $^{206}\text{Pb}/^{238}\text{U}$ age of 361.3 ± 5.9 Ma ($n = 18$, MSWD = 3.6, Fig. 3h and i), which represents the youngest age for magma eruption in the Tekesdaban region, as sample TS08 was taken from the middle of this section. This age is consistent with previously reported zircon ^{206}Pb – ^{238}U ages. Zhai *et al.* (2006) provided an age of 363.2 ± 5.7 Ma for a quartz andesite sample collected from the Axi gold mine (about 150 km north of Tekesdaban; see Fig. 1b for

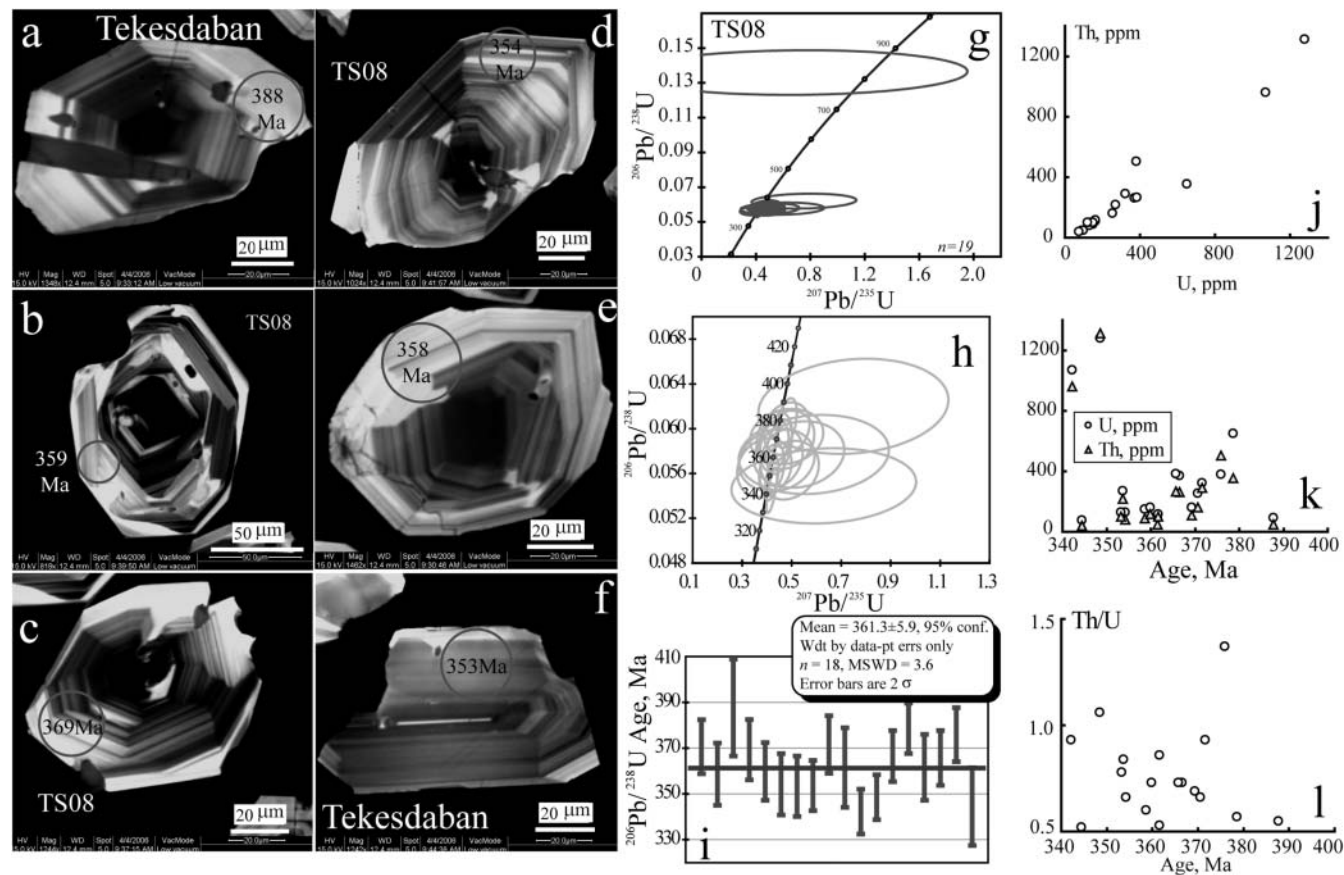


Fig. 3. (a–f) CL images of zircons from basaltic andesite in the Tekesdaban section showing the apparent U–Pb ages; (g–i) zircon SHRIMP dating results for sample TS08; (j–l) relations of U, Th and Th/U ratios for the analysed zircons.

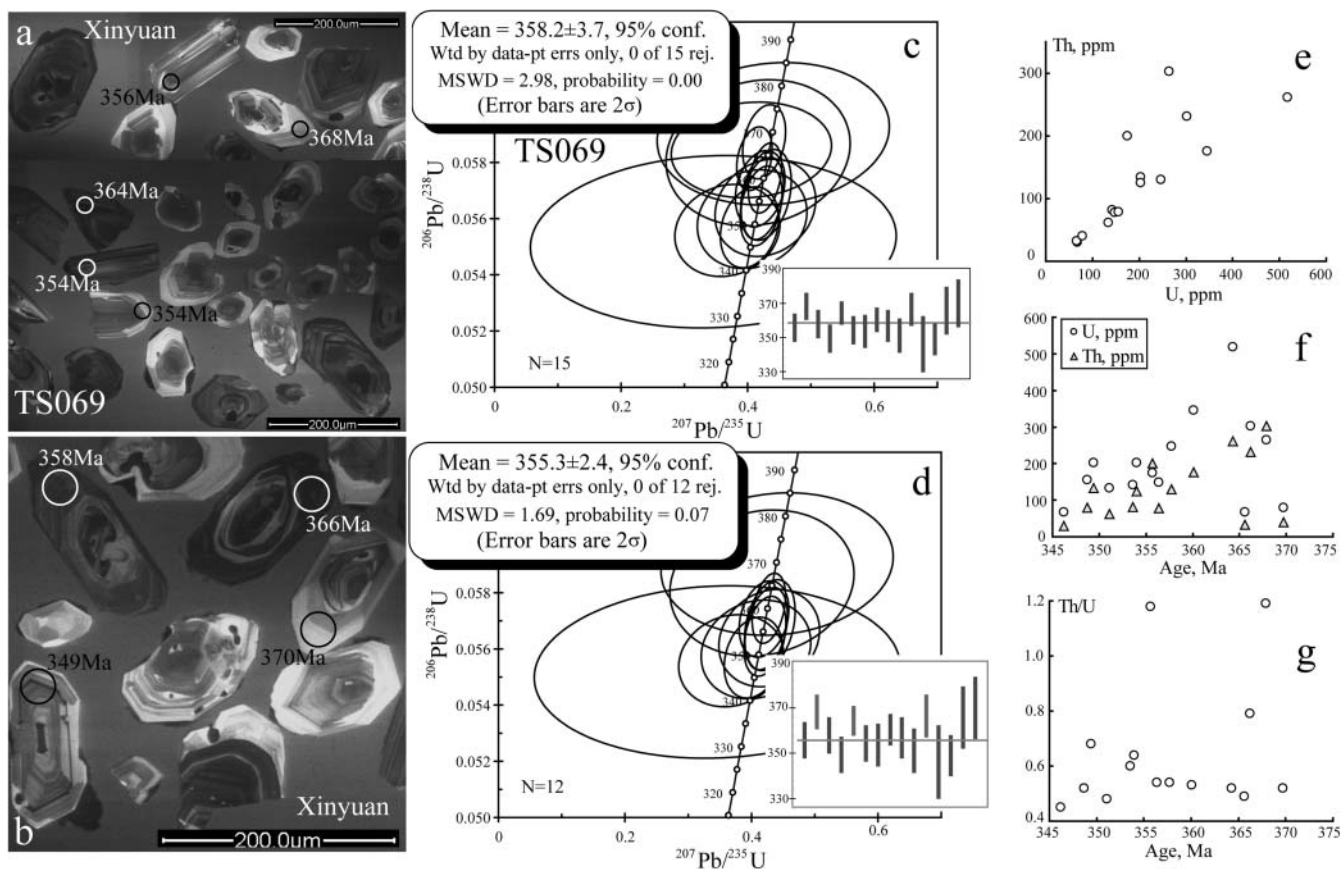


Fig. 4. (a,b) CL images of zircons from basaltic andesite in the Xinyuan section showing the apparent U–Pb ages; (c,d) SHRIMP dating results for sample TS069; (e–g) the relations of U, Th and Th/U ratios for the analysed zircons.

location). An & Zhu (2008) reported a weighted average ^{206}Pb – ^{238}U age of 386.4 ± 9.3 Ma for zircons separated from a rhyolite sample collected from a location about 20 km NW of the Axi gold mine.

Zircons from Xinyuan basaltic rocks (TS069, TS01)

Two kinds of zircon crystals (long columnar and short columnar) in basaltic andesite sample TS069 show typical magmatic zonation (Fig. 4a and b). Most zircons have cores showing magmatic zonation. Only zircon rims were dated to obtain the magma eruption time. All 15 analysed points plot on the concordia and give a weighted average $^{206}\text{Pb}/^{238}\text{U}$ age of 358.2 ± 3.7 Ma (95% confidence, MSWD = 2.98, Fig. 4c). However, apart from three analyses with obviously older apparent ages (which might represent a mixture of the zircon cores and rims, and were thus rejected), the other 12 points give a weighted average $^{206}\text{Pb}/^{238}\text{U}$ age of 355.3 ± 2.4 Ma with a higher precision (95% confidence, MSWD = 1.69, Fig. 4d). The contents of U (67–518 ppm) and of Th (32–303 ppm) are moderately variable (Fig. 4e and f). The $^{232}\text{Th}/^{238}\text{U}$ ratios of these zircons range between 0.45 and 1.19 (Fig. 4g). We suggest that the magma eruption in the Xinyuan region started at *c.* 355 Ma, because the zircons measured were separated from the bottom of the volcano-sedimentary section (see Fig. 2c).

Zircons in TS01 (basalt) are mainly prismatic in shape with magmatic zonation. Some zircons also have cores with magmatic zonation (Fig. 5a–f). The $^{232}\text{Th}/^{238}\text{U}$ ratios of these

zircons range between 0.30 and 1.28 with U concentrations of 56–697 ppm and Th concentrations of 21–531 ppm (Fig. 5j–l). Their apparent ages vary between 344 and 395 Ma. Several analyses probably reflect the mixed ages of zircon margins and cores (these zircon grains are small, and their cores and margins are not always clear). Except for eight analyses on zircon cores and the possible mixtures, the other 12 analyses give a weighted average $^{206}\text{Pb}/^{238}\text{U}$ age of 352.2 ± 3.2 Ma (95% confidence, MSWD = 1.1, Fig. 5h and i), which is consistent with the age of zircons from the underlying sample TS069 (*c.* 355 Ma).

Zircons from the Laerdundaban trachy-andesite (TS04)

A fresh trachy-andesite sample (TS04) covering the altered basalt (see Fig. 2d for location) contains inherited zircons. All inherited zircons show brighter CL images compared with the magmatic zircons in the same sample (Fig. 6a). The inherited zircons have apparent ages of 1604–1810 Ma, with one as old as *c.* 2340 Ma. Zircons with apparent $^{206}\text{Pb}/^{207}\text{Pb}$ ages of 1620–1720 Ma plot on the U–Pb concordia (Fig. 6b). These inherited zircons contain low U (20–258 ppm) and Th (12–131 ppm) with moderate Th/U ratios (0.35–0.79). The magmatic zircons in TS04 with dark CL images have high contents of U (759–4605 ppm) and Th (861–15011 ppm) with high Th/U ratios (1.17–2.95, Fig. 6e–g). Most data plot on the U–Pb concordia and give a weighted average $^{206}\text{Pb}/^{238}\text{U}$ age of 324.0 ± 4.9 Ma (95% confidence, $n = 13$, MSWD = 3.0, Fig. 6c and d).

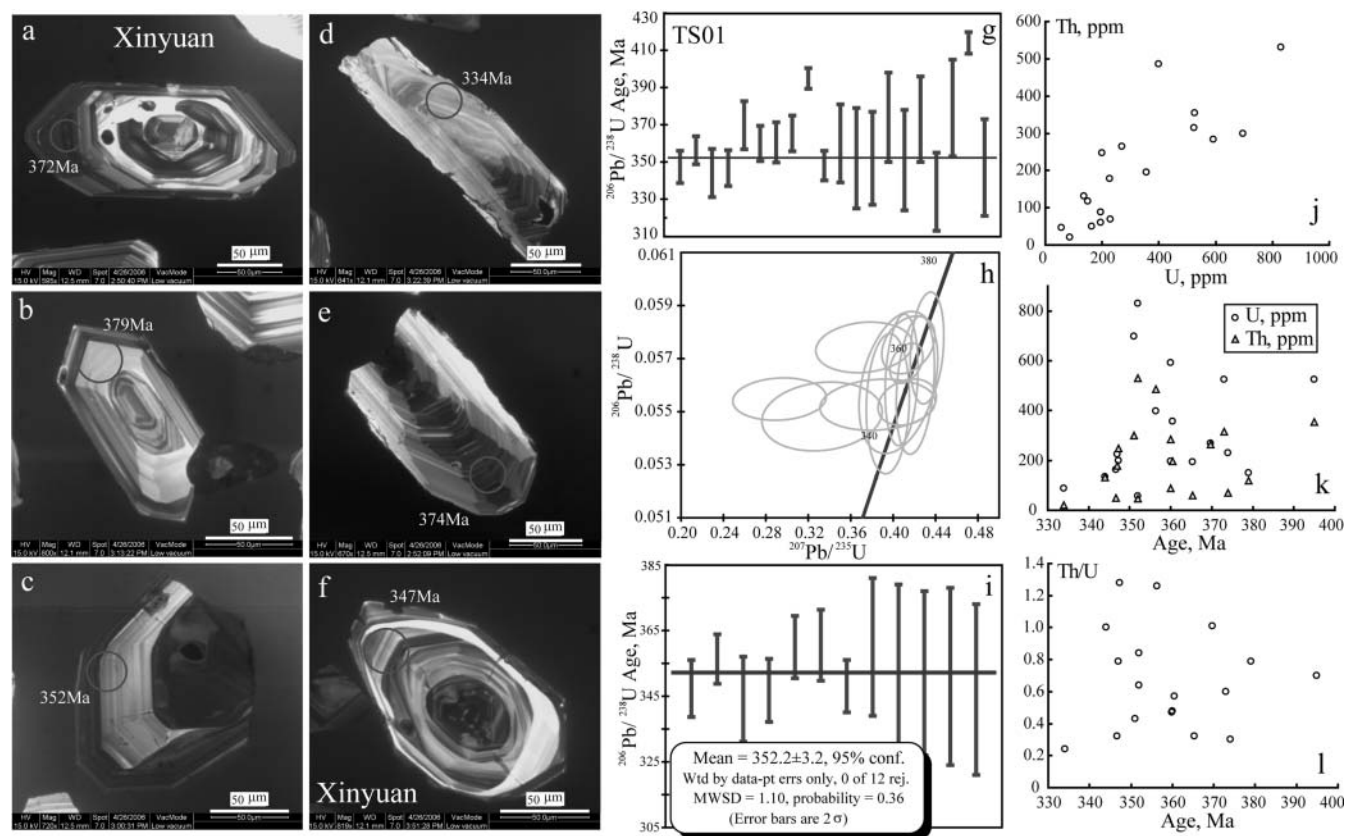


Fig. 5. (a–f) CL images of zircons from basalt in the Xinyuan section showing the apparent U–Pb ages; (g–i) SHRIMP dating results for sample TS01; (j–l) the relations of U, Th and Th/U ratios with their corresponding apparent ages for the analysed zircons.

Zircons from the Yuximolegai rhyolite (TS1618)

There are two types of zircons in the Yuximolegai rhyolite: long-columnar crystals with a clear core and rim texture (Fig. 7a–c) and euhedral grains with sector zoning (Fig. 7c–e). We tried to measure only the margins of the zircons during SHRIMP dating. Most zircons have bright CL images showing magmatic zonation with moderate U (106–740 ppm) and Th contents (79–960 ppm) with Th/U ratios of 0.57–1.38 (Fig. 7h–j). All the measured data plot on the U–Pb concordia and give a weighted average $^{206}\text{Pb}/^{238}\text{U}$ age of 316.0 ± 2.5 Ma (95% confidence, $n = 15$, MSWD = 1.9, Fig. 7f and g).

Geochemistry

Late Palaeozoic volcanic rocks in the southwestern Tianshan Mountains belong to the calc-alkaline suite, ranging from basalt to rhyolite in a total alkalis–silica (TAS) diagram (Fig. 8a). Most of these rocks are classified as high-K or medium-K series, with several trachy-andesite and trachyte samples being classified as shoshonite (Fig. 8b). Samples are grouped in three periods based on the above-described zircon SHRIMP dating results: Late Devonian (385–359 Ma), Early Carboniferous (359–318 Ma) and Late Carboniferous (318–299 Ma). The Late Devonian volcanic rocks (in the Tekesdaban and Dahalajunshan regions) range from basalt, basaltic andesite, andesite and trachy-andesite to trachyte. Samples collected from the Xinyuan section (Early Carboniferous) continuously range from basalt, basaltic andesite, basaltic trachy-andesite and andesite to trachy-andesite. The Late

Carboniferous volcanic rocks (in the Laerdundaban and Yuximolegai regions) are basaltic andesite, basaltic trachy-andesite, andesite, trachy-andesite, trachyte, dacite and rhyolite. Basaltic rocks are generally insignificant for the Late Carboniferous volcanic rock suite.

The REE distribution patterns for most of the studied samples are similar, showing obvious enrichments of light REE (LREE) and negative Eu anomalies (Fig. 9). However, the REE fractionation patterns are different for samples from different regions as well as for different rock types. Total REE contents in rock samples collected from the Tekesdaban section vary from 119 to 221 ppm with $(\text{La}/\text{Yb})_{\text{N}}$ of 6.18–9.47 and obvious negative Eu anomalies ($\text{Eu}/\text{Eu}^* = 0.68\text{--}0.83$, see Fig. 9a). Samples collected from the Dahalajunshan region have total REE contents of 94–149 ppm with obvious negative Eu anomalies ($\text{Eu}/\text{Eu}^* = 0.74\text{--}0.87$, see Fig. 9b). The REE fractionations are moderate with $(\text{La}/\text{Yb})_{\text{N}}$ of 5.0–7.2.

Samples of the Late Devonian volcanic rocks from Tekesdaban (Fig. 10a) and Dahalajunshan (Fig. 10b) exhibit similar geochemical signatures in the primitive mantle normalized spider diagrams, with obvious enrichments of large ion lithophile elements (LILE). Depletions of Nb–Ta, P and Ti also are apparent. Basalts from Dahalajunshan show no obvious Sr anomalies, whereas most basaltic andesite samples display strong Sr enrichments (Fig. 10b).

The samples from the Xinyuan section mainly consist of basaltic rocks (total REE 51.7–76.5 ppm) and andesitic rocks (total REE 60.5–155.3 ppm). The REE fractionation characteristics of basaltic samples from Xinyuan (Fig. 9c) are less variable

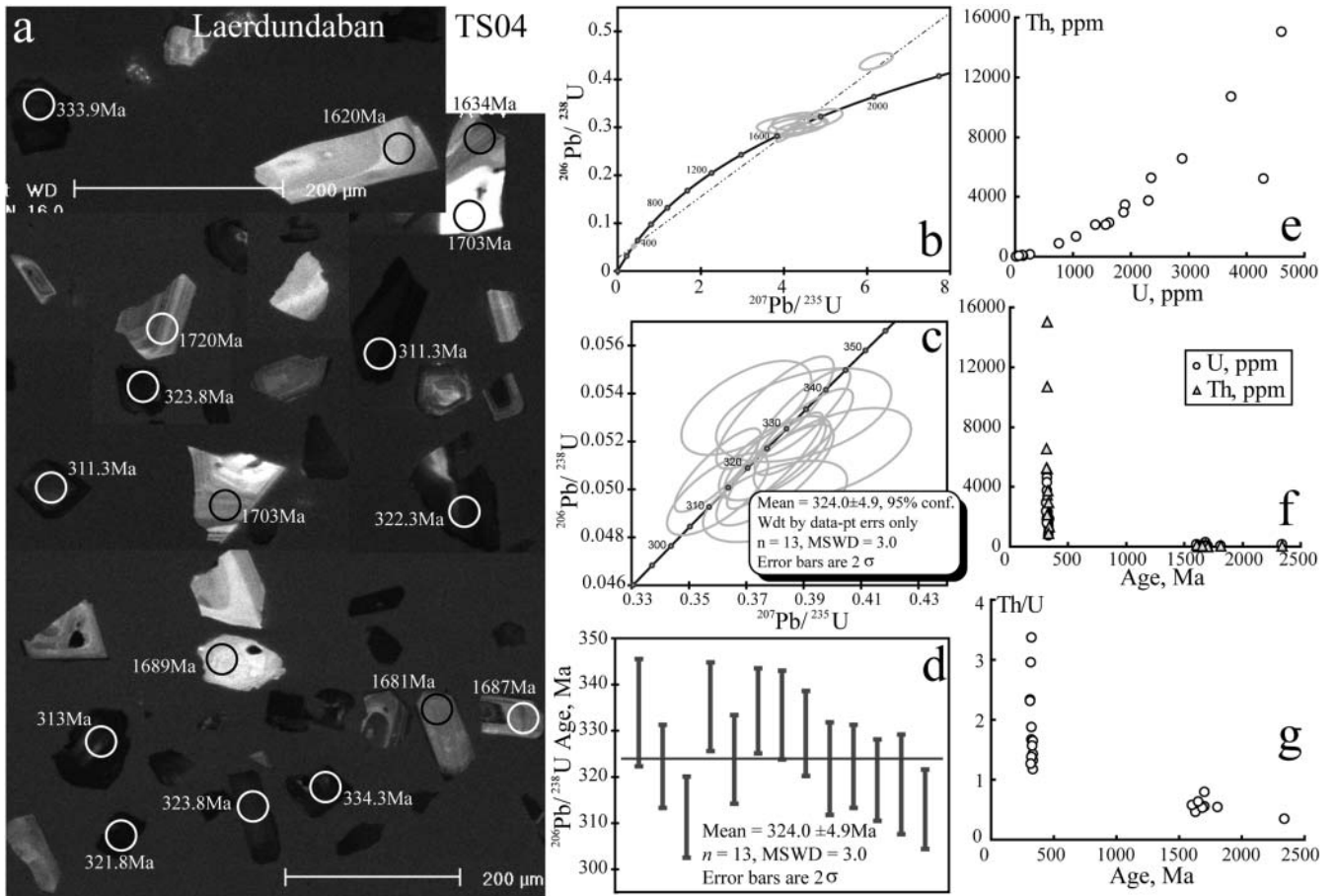


Fig. 6. (a) CL images of zircons from altered basalt in the Laerdundaban section showing the apparent U–Pb ages; (b–d) SHRIMP dating results for sample TS04; (e–g) the relations of U, Th and Th/U ratios for the analysed zircons.

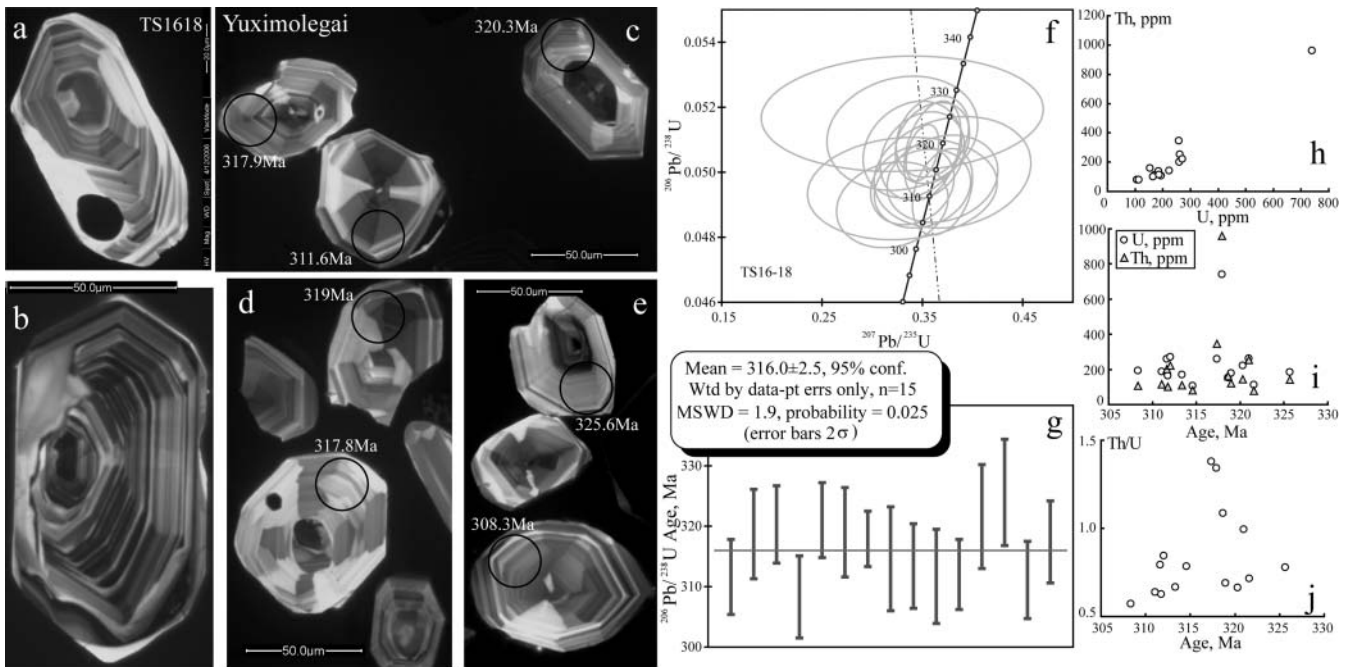


Fig. 7. (a–e) CL images of zircons from trachy-andesite in the Yuximolegai rhyolite sample showing the apparent U–Pb ages; (f,g) SHRIMP dating results for sample TS1618 from Yuximolegai rhyolite; (h–j) the relations of U, Th and Th/U ratios for the analysed zircons.

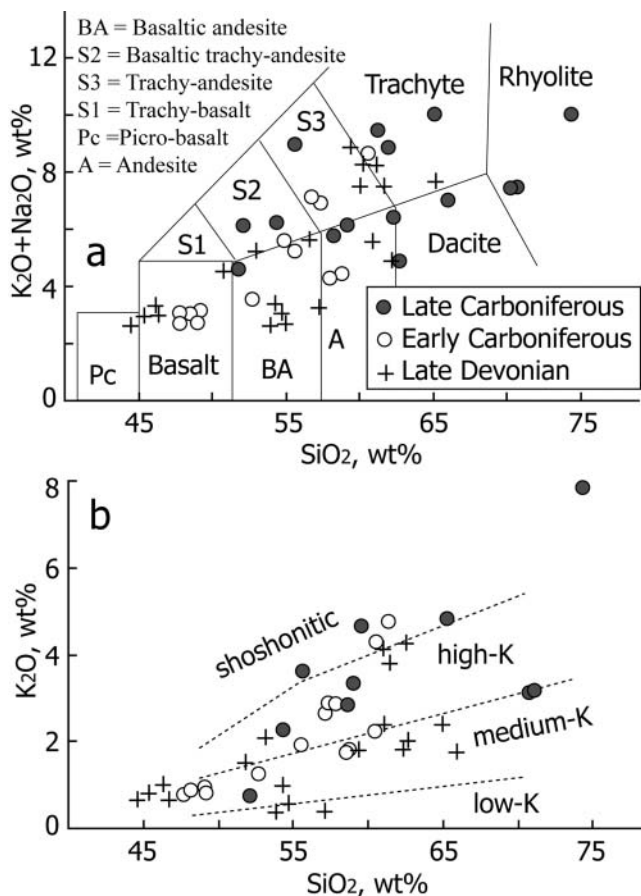


Fig. 8. (a) Classification of the Late Palaeozoic volcanic rocks in terms of TAS; (b) plot of SiO₂ v. K₂O for Late Palaeozoic volcanic rocks in the southwestern Tianshan Mountains.

than those of the andesitic samples (Fig. 9d). The Xinyuan basaltic samples have variable (La/Yb)_N values (3.34–4.92) with weak negative Eu anomalies (Eu/Eu* = 0.83–0.87, Fig. 9c). Andesitic samples have moderately variable (La/Yb)_N values of 3.75–7.92 and weak negative Eu anomalies (total REE = 60.5–94.7 ppm, Eu/Eu* = 0.86–0.93) with one exception (TS096, (La/Yb)_N = 7.9, total REE = 155.3 ppm, Eu/Eu* = 0.72, Fig. 9d). The primitive mantle normalized spider diagrams for the Xinyuan samples are shown in Figure 10c and d. The Xinyuan basaltic rocks are moderately enriched in LILE with obvious depletion in Nb and Ta (Fig. 10c). The andesitic samples show strong enrichments of LILE with depletions of Nb, P and Ti (Fig. 10d).

Samples from the Laerdundaban section mainly consist of trachyte, basaltic trachy-andesite, trachy-andesite and rhyolite. One rhyolite sample (TS191) is obviously enriched in REE (total REE *c.* 200 ppm) with an obvious negative Eu anomaly (Eu/Eu* = 0.73, see Fig. 9e), whereas other samples (total REE 65.3–149 ppm) with negative Eu anomalies (Eu/Eu* = 0.64–0.97) show moderate fractionation of REE with (La/Yb)_N values of 2.64–6.09. The primitive mantle normalized spider diagram for these volcanic rocks shows strong LILE enrichments with Nb and Ti valleys (Fig. 10e).

Samples from the Yuximolegai region consist of rhyolite, dacite and andesite. One andesite sample (TS022) has an extremely high total REE content (178 ppm) relative to rhyolite

(TS017, total REE = 90.6 ppm). Both andesite and rhyolite samples show enrichments of LREE with strong negative Eu anomalies (Fig. 9f). The primitive mantle normalized spider diagrams for the Yuximolegai rhyolite and andesite samples are highly variable. All samples show Nb and Ti valleys and enrichments of Cs, Rb, Th and U (Fig. 10f).

The Sr–Nd isotopic compositions of the representative volcanic rock samples in the southwestern Tianshan Mountains are shown in Figure 11a. The Late Devonian basaltic samples have negative $\epsilon_{\text{Nd}(T)}$ values (–5.16 to –3.07) and high initial ⁸⁷Sr/⁸⁶Sr ratios (0.7073–0.7098), whereas the Carboniferous volcanic rocks have positive $\epsilon_{\text{Nd}(T)}$ values with one exception (TS096, $\epsilon_{\text{Nd}(T)}$ = –0.18). The Late Carboniferous volcanic rocks have relatively higher $\epsilon_{\text{Nd}(T)}$ values (+5.89 to +2.79) and lower initial ⁸⁷Sr/⁸⁶Sr ratios (0.7032–0.7054) than the Early Carboniferous samples. A trend from the Late Devonian to Late Carboniferous is apparent. The Late Devonian volcanic rocks (in the western part of the southwestern Tianshan Mountains) show enriched geochemical signatures with high initial ⁸⁷Sr/⁸⁶Sr ratios and negative $\epsilon_{\text{Nd}(T)}$ values, whereas the Late Carboniferous volcanic rocks (in the eastern part of the southwestern Tianshan Mountains) all plot in the depleted mantle region, and the Early Carboniferous samples plot between the Late Devonian basaltic rocks and the Late Carboniferous samples in the graph of initial ⁸⁷Sr/⁸⁶Sr ratios v. $\epsilon_{\text{Nd}(T)}$ values.

Lu–Hf isotopic composition of zircons

The Lu–Hf isotopic compositions of the zircon rims were analysed to constrain the magma source of the Late Palaeozoic volcanic rocks in the southwestern Tianshan Mountains. The Lu–Hf isotope analysis results are shown in Figure 12. The $\epsilon_{\text{Hf}(T=361\text{Ma})}$ values vary from +2.8 to +15.6 with a weighted average value of +9.5 (*n* = 33, Fig. 12a) for zircons from the Tekesdaban basaltic andesite. Their initial ¹⁷⁶Hf/¹⁷⁷Hf is 0.28263–0.28299. The $\epsilon_{\text{Hf}(T=352\text{Ma})}$ values vary from +1.5 to +15.6 with a weighted average value of +8.9 (*n* = 19, Fig. 12b) for zircons from the Xinyuan basaltic samples (with initial ¹⁷⁶Hf/¹⁷⁷Hf of 0.28260–0.28299). The $\epsilon_{\text{Hf}(T=313-316\text{Ma})}$ values vary from +1.4 to +14.6 with a weighted average value of +10.3 (*n* = 6, Fig. 12c) for zircons from the Laerdundaban trachy-andesite (initial ¹⁷⁶Hf/¹⁷⁷Hf = 0.28262–0.28299). For comparison, the $\epsilon_{\text{Hf}(T>470\text{Ma})}$ values for some old zircons are also shown in Figure 12d. The old (inherited) zircons have obviously low $\epsilon_{\text{Hf}(T>470\text{Ma})}$ values (from –0.7 to –5.5), indicating that the inherited zircons are different in origin from the Late Palaeozoic volcanic zircons, which probably represent the relics of old continental crust recycled into the studied magma sources.

Discussion

Time constraint for volcanic arc related to the Palaeo-southern Tianshan Ocean subduction

A northward subduction of the Palaeo-southern Tianshan Ocean beneath the Yili terrane during Devonian to Carboniferous time terminated the convergent phases of mountain building in the southwestern Tianshan Mountains (Gao *et al.* 1998; Zhang *et al.* 2003). The recently identified Silurian–Devonian active-margin deep-marine systems and palaeogeography in the Alai Range of the southwestern Tianshan Mountains (Pickering *et al.* 2008) have provided additional evidence that the Palaeo-southern Tianshan Ocean subducted northwards beneath the Yili terrane during the Devonian period.

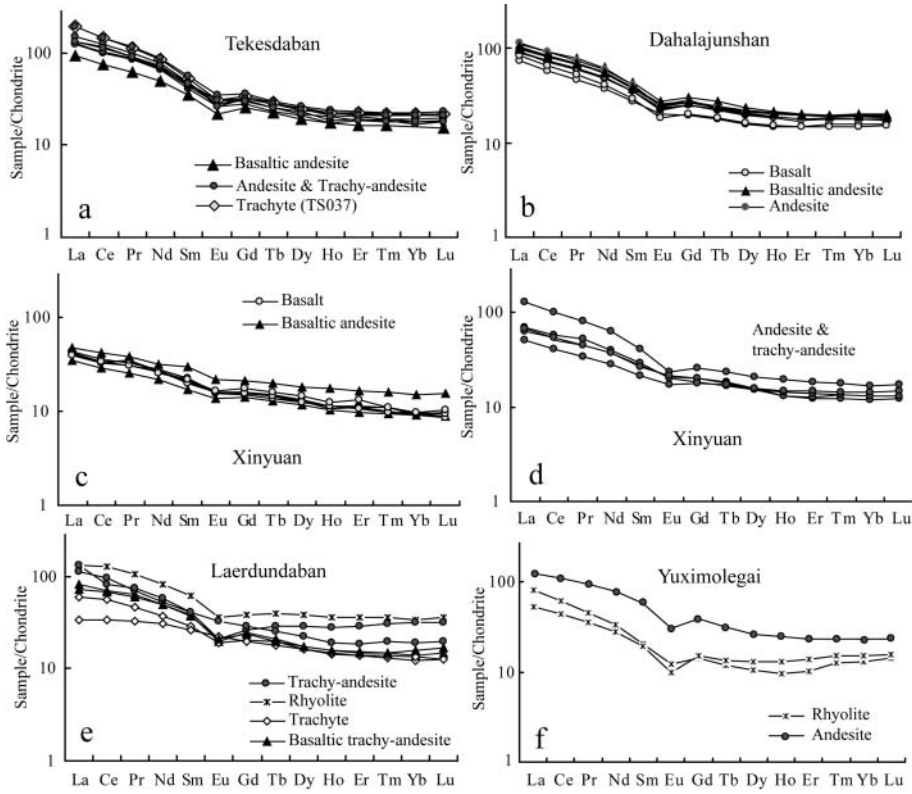


Fig. 9. REE distribution patterns for the Late Palaeozoic volcanic rocks in the southwestern Tianshan Mountains.

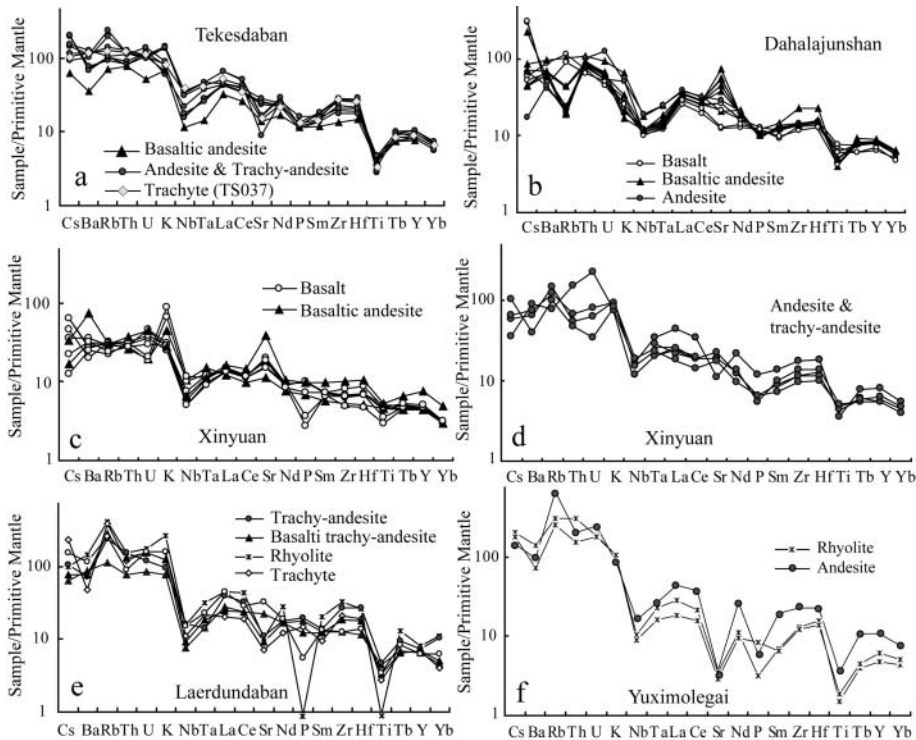


Fig. 10. Primitive mantle normalized spider diagrams for the Late Palaeozoic volcanic rocks in the southwestern Tianshan Mountains. The primitive mantle data are taken from Sun & McDonough (1989).

In the southwestern part of the southwestern Tianshan Mountains (Tekesdaban region), the section along a national road (Fig. 1b) exposes neither the bottom nor the top of the volcano-sedimentary suite (Fig. 2a). Zircon sample TS08 separated from basaltic andesite was collected from the middle part of this section. Thus, the zircon ^{206}Pb – ^{238}U age of the sample TS08

(361.3 ± 5.9 Ma, Fig. 3h and i) indicates only that the magma eruption occurred before c. 361 Ma (Late Devonian).

Zircons (TS069, TS01) were separated from the bottom of a volcano-sedimentary section roughly 10 km thick (see Fig. 2c). The ^{206}Pb – ^{238}U ages of these zircons (355–352 Ma, see Figs 4c,d and 5h,i) imply that the magma eruption occurred in the

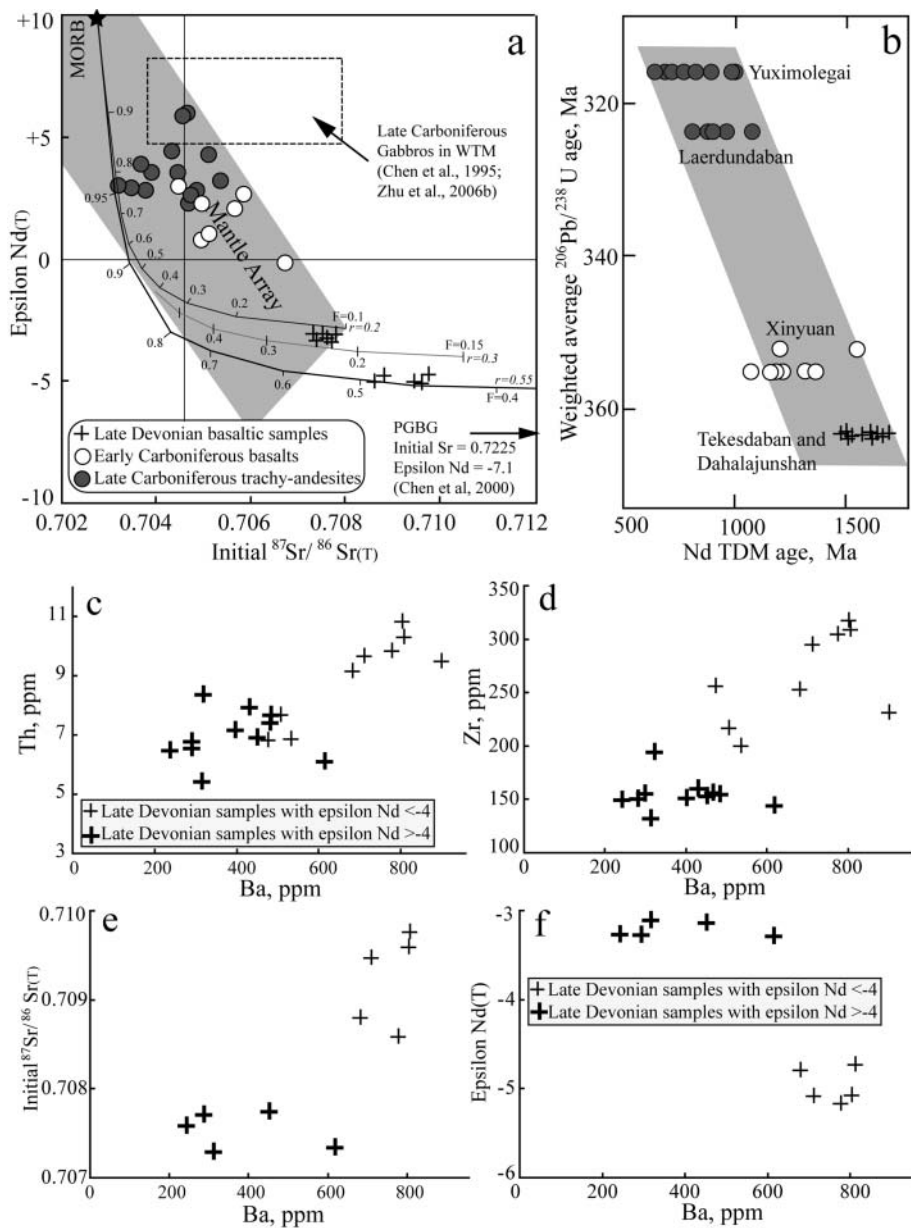


Fig. 11. (a) Plot of initial $^{87}\text{Sr}/^{86}\text{Sr}$ v. $\epsilon_{\text{Nd}}(\text{T})$ for Late Palaeozoic volcanic rocks in the southwestern Tianshan Mountains. Late Carboniferous gabbros that intruded the Late Devonian to Carboniferous volcanic sedimentary rocks in the southwestern Tianshan Mountains (from Chen *et al.* 1995; Zhu *et al.* 2006b) are included for comparison. The curve marked with numbers are AFC (DePaolo 1981) calculation results with $F = 0.10, 0.15$ and 0.4 . Proterozoic gneissic biotite granite (PGBG) in the southwestern Tianshan Mountains (from Chen *et al.* 2000) is assumed to represent the continental crust; MORB is assumed to represent the depleted mantle. (b) Plot showing the variation trend between the zircon ^{206}Pb – ^{238}U ages and the T_{DM} ages of Nd isotopes. (c,d) Plots showing the variations of Ba contents v. Th (c) and Zr (d) contents in the Late Devonian basaltic samples. (e,f) Plots showing the variations of Ba contents v. initial $^{87}\text{Sr}/^{86}\text{Sr}$ ratios (e) and ϵ_{Nd} values (f) of the Late Devonian basaltic samples.

Early Carboniferous in the central part of the southwestern Tianshan Mountains.

A layer thicker than 6000 m, mainly consisting of volcanic rocks, directly covers the Silurian gneisses and schist (Fig. 2d) in the eastern part of the southwestern Tianshan Mountains (Laerdundaban region). Sample TS04 represents zircons from a trachy-andesite collected at the section bottom (see Fig. 2d for location). The zircon ^{206}Pb – ^{238}U age of this sample (324 ± 4.9 Ma, Fig. 6c and d) thus represents the late stage of magma eruption in the Laerdundaban region. We earlier reported a zircon ^{206}Pb – ^{238}U age of 312.8 ± 4.2 Ma (sample TS02, MSWD = 1.7, Zhu *et al.* 2005). That sample was collected from c. 500 m higher in the same section (see Fig. 1f for location). The magma eruption in the Laerdundaban region therefore lasted until c. 313 Ma or later.

The Yuximolegai region, locating to the north of the Laerdundaban region, is mainly covered by Carboniferous rhyolite, andesite, tuff and clastic sedimentary rocks. The zircon

^{206}Pb – ^{238}U age of sample TS1618 separated from rhyolite (316.0 ± 2.5 Ma, Fig. 7f and g) represents the late stage of magma eruption in the eastern part of the southwestern Tianshan Mountains.

Therefore, the time span of the studied volcanic rocks in the southwestern Tianshan Mountains is large (>361 Ma to c. 313 Ma), which suggests that the Late Palaeozoic volcanic eruptions in the southwestern Tianshan Mountains occurred at different times (in different regions). The magmatic activity in the western part of the southwestern Tianshan Mountains was earlier (Late Devonian) than that in the eastern part (Early Carboniferous to Late Carboniferous). The variation in time and space of the volcanic rocks in the southwestern Tianshan Mountains indicates that the magma eruptions started in the western part of the southwestern Tianshan Mountains (e.g. Tekesdaban, Dahalajunshan) during the Late Devonian. Volcanic activity in the central part of the southwestern Tianshan Mountains (e.g. Xinyuan) occurred during the Early Carboni-

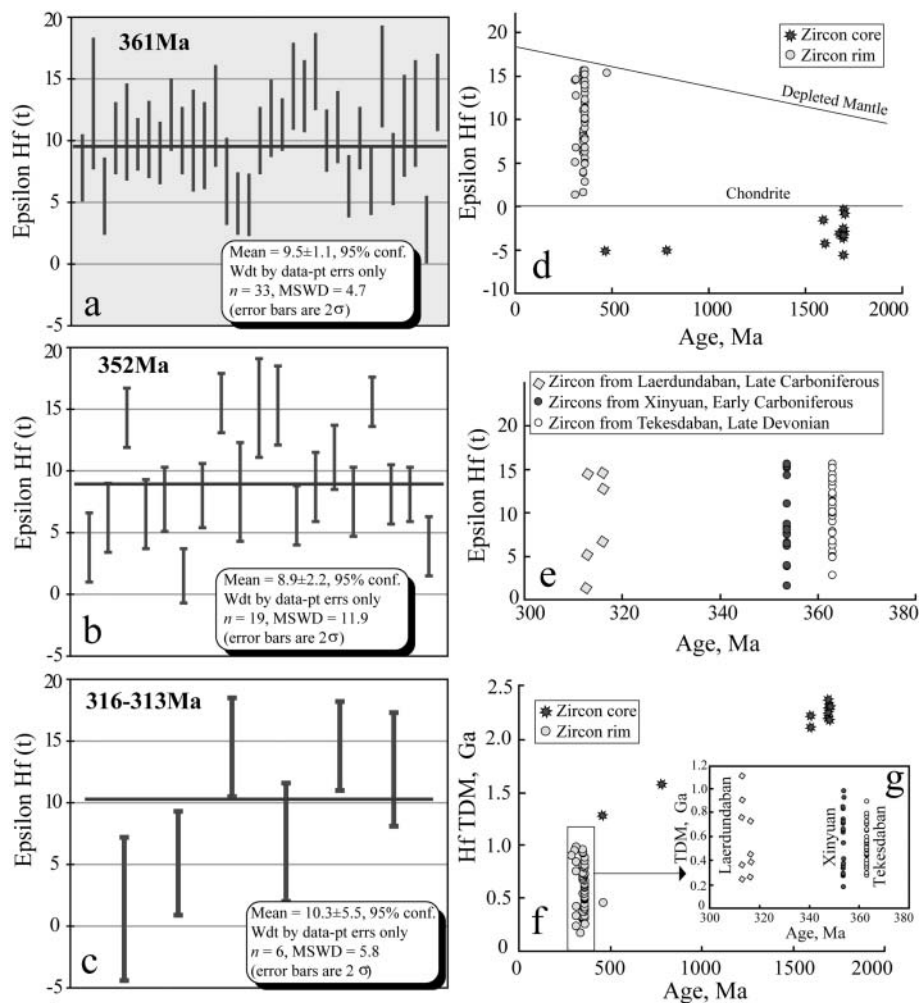


Fig. 12. (a–c) Plots showing the weighted average values of the $\epsilon_{\text{Hf}}(t)$ for Late Devonian (361 Ma; **a**), Early Carboniferous (352 Ma; **b**) and Late Carboniferous (316–313 Ma; **c**) zircons from the Late Palaeozoic volcanic rocks in the southwestern Tianshan Mountains; (**d–g**) Hf isotopic compositions and the T_{DM} values of zircons from the Late Palaeozoic volcanic rocks in the southwestern Tianshan Mountains. The $\epsilon_{\text{Hf}}(t)$ of each zircon was calculated at its U–Pb age. The T_{DM} values were calculated following Yang *et al.* (2006).

ferous (*c.* 355 Ma). In the eastern part of the southwestern Tianshan Mountains (Laerdundaban–Yuximolegai), the magmatic eruptions did not occur until the Late Carboniferous (<324–313 Ma), and mostly formed trachy-andesite, andesite, trachyte and rhyolite. This time–space trend suggests a volcanic chain, progressing from the western (in the Late Devonian) to the eastern part (in the Late Carboniferous) of the southwestern Tianshan Mountains. This >600 km long volcanic chain does not end at the border between China and other countries (Kazakhstan, Kyrgyzstan); similar volcanic rocks in Kazakhstan and Kyrgyzstan dated as Late to Early Devonian have been reported (Volkova & Budanov 1999; Maksumova *et al.* 2001; Kurchavov *et al.* 2002; Morozov & Talitskii 2006). Thus the southwestern Tianshan Mountains extends to Kyrgyzstan, Tajikistan and Kazakhstan, and connects the Atbashi, Fan–Karategin and Bashijier–Xierpuhov Devonian volcanic belts.

The geochemistry of trace elements demonstrates that the studied volcanic rocks are typical of continental arc magmatism. The data presented here suggest that the Devonian–Carboniferous volcanic rocks in the southwestern Tianshan Mountains, mainly consisting of basalt, trachyte, trachy-andesite, andesite and rhyolite, represent the continental arc formed during the subduction of the Palaeo-southern Tianshan Ocean during Late Devonian to Carboniferous times. The southwestern Tianshan Mountains represent the continental margin of the Yili terrane during the formation of the Late Palaeozoic volcanic rocks.

During that period, the Palaeo-southern Tianshan Ocean continued its subduction northwards.

The zircon ^{206}Pb – ^{238}U ages, the T_{DM} ages of Hf isotopes for zircons and the T_{DM} ages of Nd isotopes for the whole-rock samples are inconsistent. Figure 11b displays the variations of the Nd T_{DM} ages for the whole-rock samples versus the weighted average $^{206}\text{Pb}/^{238}\text{U}$ ages of zircons separated from the studied whole-rock samples. The Nd T_{DM} ages of the whole-rocks (637–1705 Ma) are apparently older than the zircon $^{206}\text{Pb}/^{238}\text{U}$ ages (313–361.3 Ma, see Figs 3–7). A trend can be roughly identified, as the rock age decreases with the decrease of the Nd T_{DM} ages (see Fig. 11b). This trend probably reflects the geochemical signatures of magma sources in different regions (from the western to the eastern part of the southwestern Tianshan Mountains) and at different times (from Late Devonian to Late Carboniferous). The Nd T_{DM} ages for the Yuximolegai samples (637–991 Ma) and the Laerdundaban samples (806–1071 Ma) are similar, and both differ from those of the Xinyuan samples (1054–1538 Ma), the Tekesdaban samples (1508–1695 Ma) and the Dahalajunshan samples (1578–1705 Ma). The Late Carboniferous magma source has a Neoproterozoic Nd T_{DM} age. The Early Carboniferous magma source has a Mesoproterozoic Nd T_{DM} age. The magma source of the Late Devonian volcanic rocks has a Mesoproterozoic to Palaeoproterozoic Nd T_{DM} age. The large time span of the Nd T_{DM} ages implies a mixture of different magma sources, as the T_{DM} age of the Nd isotopes reflects the time when magma separated from the depleted mantle.

Figure 12f displays the inherited zircon cores with much older Hf T_{DM} ages relative to the Late Palaeozoic zircons in the southwestern Tianshan Mountains. All the inherited zircons are characterized by negative ϵ_{Hf} values. Most zircons crystallized in the studied volcanic rocks have Hf T_{DM} ages of 0.4–0.8 Ga (with no relation to their $^{206}Pb/^{238}U$ ages, see Fig. 12f and g). The Hf T_{DM} ages (0.92–0.36 Ga for zircons with $^{206}Pb/^{238}U$ ages of <361.3 Ma) are generally younger than the Nd T_{DM} ages (1.70–0.71 Ga), which suggests that Hf isotope geochemistry of the Late Palaeozoic magmatic zircons represents only the geochemical signatures of the corresponding magma at its early evolution stage, because zircon generally is an early phase crystallized in magma at high temperature, whereas the Nd isotopes of the whole-rock samples represent the total results of the magma evolution, during which time continental crust was assimilated for the Late Devonian samples at least (see below). Consequently, magmatic rocks become enriched relative to the mineral phase crystallized at early stage. Thus, the high positive ϵ_{Hf} values (weighted average values of +9.5, +8.9 and +10.3 for Late Devonian, Early Carboniferous and Late Carboniferous samples, respectively; see Fig. 12e) of the studied zircons suggest that the magma originated from a depleted mantle.

Magma source of the Late Devonian volcanic rocks

The differences between the Sr and Nd isotope compositions of the basaltic and andesitic rocks rule out a single origin of each whole assemblage by simple fractional crystallization and strongly support the occurrence of open-system processes for the Devonian volcanic rocks in the southwestern Tianshan Mountains. The rocks with low ϵ_{Nd} and high initial $^{87}Sr/^{86}Sr$ values could be produced by a combination of continental crust and mantle, as suggested by many researchers (Hart 1988). The AFC model is used to explain the isotope characteristics of the Late Devonian volcanic rocks in the southwestern Tianshan Mountains. In the AFC calculations, F represents the ratio of residual magma mass to the initial magma mass. The lower the value of F the greater the fractional crystallization. The value of r represents the ratio of assimilated wall-rocks to the rate at which fractionating phases are being effectively separated from the magma. The larger the r values the stronger the assimilation process. This value may be changing continuously as magma moves through the continental crust. D_{Sr} and D_{Nd} represent the bulk solid–liquid partition coefficient between the fractionating crystalline phases and the magma for Sr and Nd, respectively. Based on the distribution coefficients of Sr and Nd (see Rollinson (1993) for a summary of distribution coefficients) and the mineral phases of the Late Devonian basaltic rocks, $D_{Sr} = 1.5$ and $D_{Nd} = 0.12$ were used in the AFC calculations. A depleted mid-ocean ridge basalt (MORB)-type magma is assumed in the AFC calculations. The MORB ($\epsilon_{Nd} = 10$, initial $^{87}Sr/^{86}Sr = 0.7020$) and the Proterozoic gneissic biotite granite in the southwestern Tianshan Mountains ($\epsilon_{Nd(T)} = -7.1$, initial $^{87}Sr/^{86}Sr(T) = 0.7225$, U–Pb age of 707 Ma, Chen *et al.* 2000) are assumed to represent the end-member of the mantle wedge and the continental crust, respectively. The compositions of the Late Devonian basaltic rocks can be modelled by the AFC process with end-members of depleted mantle and Proterozoic gneissic biotite granite (see Fig. 11a).

The Late Devonian basaltic rocks are characterized by negative ϵ_{Nd} and high initial $^{87}Sr/^{86}Sr$ values, and apparently fall into two groups in a plot of ϵ_{Nd} v. initial $^{87}Sr/^{86}Sr$ (Fig. 11a). The group I samples (trachy-andesite, trachyte and basaltic andesite) have lower $\epsilon_{Nd(T)}$ values (<–4.0) and higher initial $^{87}Sr/^{86}Sr(T)$

ratios (>0.708). The group II samples, with higher $\epsilon_{Nd(T)}$ values and lower initial $^{87}Sr/^{86}Sr(T)$ ratios, consist of basalts and basaltic andesite. AFC calculation shows that the group II samples underwent low-degree contamination by Proterozoic gneissic biotite granite ($r = 0.22$ – 0.27 , $F = 0.12$ – 0.22), whereas the group I samples have been significantly contaminated by the continental crust represented by Proterozoic gneissic biotite granite ($r = 0.49$ – 0.55 , $F = 0.40$ – 0.49).

The contamination of the magma source of the Late Devonian magma by the continental crust also is shown by the behaviour of trace elements. The group I samples are especially enriched in Ba (mostly higher than 400 ppm) relative to the group II samples. Both Ba and Th are highly concentrated in Proterozoic gneissic biotite granite (Th = 19 ppm, Ba = 1185 ppm, Chen *et al.* 2000). The positive correlation between Ba and Th for the Late Devonian volcanic rocks (Fig. 11c) suggests that the basaltic magma contains relatively low Th and Ba compared with the andesitic magma. The magma corresponding to the Late Devonian andesitic samples contains apparent higher Zr compared with the basaltic samples (Fig. 11d). This is related to the partial melting of zircons in Proterozoic gneissic biotite granite (as well as in the sedimentary rocks). The addition of these zircons in magma could provide a reasonable interpretation for the higher Zr contents (see Fig. 11d) in the studied Late Devonian volcanic rocks with lower $\epsilon_{Nd(T)}$ values. The inherited zircons occurring in the studied volcanic rocks have negative $\epsilon_{Hf(T)}$ values (–0.7 to –5.1, see Fig. 12d). The addition of continental materials with such zircons to the magma source would apparently decrease the $\epsilon_{Nd(T)}$ values of the whole-rocks but would not greatly affect the $\epsilon_{Hf(T)}$ values of the newly crystallized zircons. Zircons in Proterozoic gneissic biotite granite should be the last melted phase. This implies that the high Zr concentrations in the Late Devonian andesitic samples correspond to a higher degree of partial melting of Proterozoic gneissic biotite granite compared with the basaltic samples (with lower Zr concentrations, see Fig. 11d). Consequently, the AFC process was weak for the basaltic magma compared with the andesitic magma (see Fig. 11a). The higher degree of AFC for the group I samples is consistent with the significant partial melting of the continental crust.

The crystallization of the magmatic zircons in the Late Devonian andesitic rocks occurred at an early stage of the AFC process, when the zircons in country rocks still were not melted but most of the other mineral phases of the country rocks had been partially melted. That is why most of the $\epsilon_{Hf(T)}$ values obtained from the Late Devonian zircons are positive whereas only the inherited zircon cores have negative $\epsilon_{Hf(T)}$ values (see Fig. 12d). The increased assimilation of country rocks (Proterozoic gneissic biotite granite as well as sedimentary rocks) caused the enrichments (low $\epsilon_{Nd(T)}$ values, high $^{87}Sr/^{86}Sr(T)$ ratios, high Ba and Th contents, Fig. 11a and c).

Magma source of the Carboniferous basaltic rocks

The Carboniferous volcanic rocks in the southwestern Tianshan Mountains plot in the mantle array in a graph of $^{87}Sr/^{86}Sr$ v. $\epsilon_{Nd(T)}$ (Fig. 11a). These Carboniferous magmatic rocks are characterized by high $\epsilon_{Nd(T)}$ values (–0.18 to +5.95) and variable initial $^{87}Sr/^{86}Sr$ ratios (0.7032–0.7054). The high field strength element (HFSE) pairs (e.g. Nb–Ta and Zr–Hf) are generally thought to exhibit concordant geochemical behaviour during mantle melting. Similar to most Late Devonian samples, the $(Nb/Ta)_N$ ratios of most Carboniferous samples are <1.0 whereas the $(Zr/Hf)_N$ values are close to 1.0. The strong Nb–Ta fractiona-

tion (most $(\text{Nb}/\text{Ta})_N < 0.8$) might be caused by mantle alteration as a result of subduction fluid. This is indicated also by the enrichments of LILE and depletions of Nb and Ti in the primitive mantle normalized plots for basaltic (Fig. 10c), andesitic and rhyolite samples in the southwestern Tianshan Mountains (see Fig. 10d–f). The AFC process in the Carboniferous magma could be negligible, based on the positive $\epsilon_{\text{Nd}(T)}$ values and low initial $^{87}\text{Sr}/^{86}\text{Sr}$ ratios (see Fig. 11a), with one exception (sample TS096, $\epsilon_{\text{Nd}(T)} = -0.18$, $\text{Ba} = 627.7$ ppm; this sample probably has been contaminated by Proterozoic gneissic biotite granite). This exception and the highly variable $\epsilon_{\text{Hf}(T)}$ values (+14.5 to +1.4) for zircons in sample TS02 with ages of 313–316 Ma suggest that continental crustal contamination might be heterogeneous for the Late Carboniferous volcanic rocks.

The degree of partial melting corresponding to the primitive rock samples in the southwestern Tianshan Mountains can be characterized using REE abundances and ratios. Highly incompatible La and less incompatible Sm abundances in basalts should constrain bulk source composition, as their contents would not be controlled by spinel- and garnet-bearing source mineralogy (Aldanmaz *et al.* 2000; Green 2006). The primitive rocks in the southwestern Tianshan Mountains have La abundances and La/Sm ratios greater than those generated by melting of either a depleted mantle or a primitive mantle composition (Fig. 13a). Similar to the subduction-modified Garibaldi volcanic belt (Green 2006), the partial melting trajectories that coincide with the basaltic rocks in the southwestern Tianshan Mountains imply 5–20% partial melting of the mantle source characterized by La abundances and La/Sm ratios enriched relative to the primitive mantle or enriched (E)-MORB. Calculations show that the Carboniferous basaltic rocks in the southwestern Tianshan Mountains correspond to a partial melting of 8–20% enriched mantle rocks (see Fig. 13a). The magma source could be further constrained as garnet–spinel lherzolite in the plot of Yb v. La/Yb (Fig. 13b). With garnet–spinel lherzolite as magma source, the magma of Early Carboniferous basaltic rocks could be produced by partial melting of 12–19% ($F = 0.12$ – 0.19), and the Late Carboniferous basaltic trachy-andesite could be produced by a relatively low degree of partial melting (8–9%, Fig. 13b).

General implications

The studied Late Devonian to Late Carboniferous volcanic rocks in the southwestern Tianshan Mountains have widely scattered geochemical and petrological characteristics that formed in a continental arc environment. Our results indicate that we have to be cautious in trying to constrain tectonic environments based on geochemical characteristics of magmatic rocks. For example, the Late Devonian zircons from the southwestern Tianshan Mountains volcanic rocks, with variable $\epsilon_{\text{Hf}(T)}$ values of +2.8 to +15.6 (weighted average +9.5, Fig. 12a), suggest that the magma should be generated from a depleted mantle, whereas the whole-rock samples of the Late Devonian basaltic rocks have negative $\epsilon_{\text{Nd}(T)}$ values of -5.16 to -3.07 with an average of -4.06 ($n = 10$) and high initial $^{87}\text{Sr}/^{86}\text{Sr}$ ratios (0.7073–0.7098, see Fig. 11a), suggesting an enriched magma source. Such a paradox is probably a general feature of the geochemical nature of magmatic rocks formed in a continental arc. The implication of this work is serious, as conclusions based solely on Sr–Nd isotopic compositions could be wrong at least for island arc magmatic rocks. Magma generated in the southwestern Tianshan Mountains continental arc has been contaminated by continental crustal materials in different places (at different time) to different degrees.

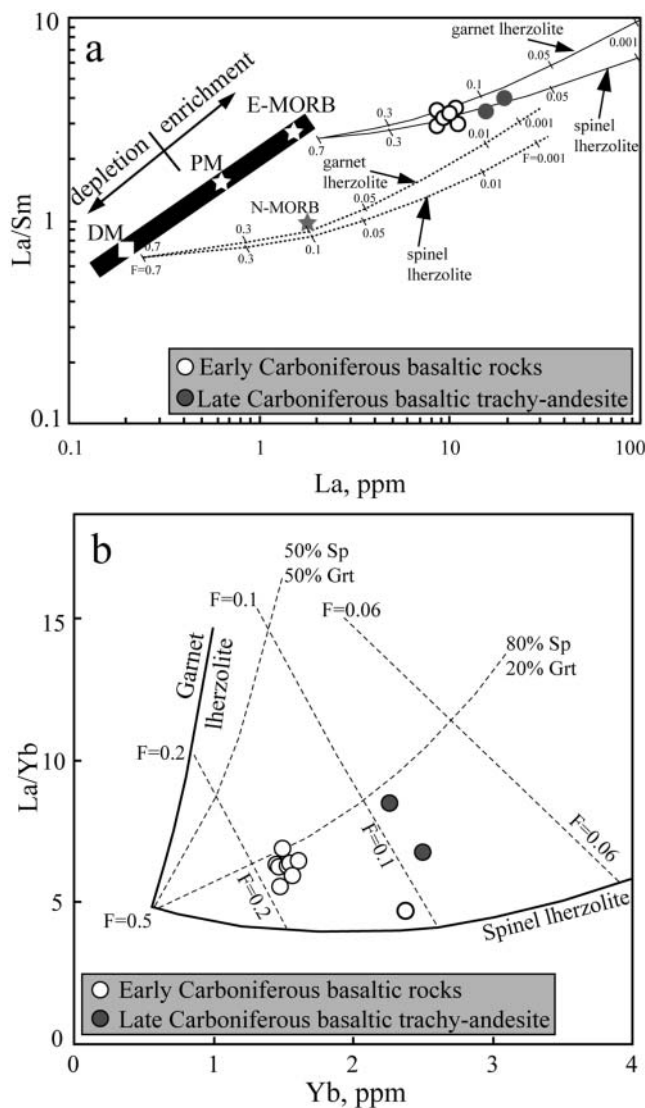


Fig. 13. (a) Plot of La v. La/Sm for the Carboniferous basaltic rocks in the southwestern Tianshan Mountains. Mantle array (bold line) defined by depleted mantle (DM; McKenzie & O’Nions 1991), primitive mantle (PM) and E-MORB compositions (based on Sun & McDonough 1989). Melting curves (lines) for spinel lherzolite (ol53 + opx27 + cpx17 + sp11) and garnet peridotite (ol60 + opx20 + cpx10 + gt10) sources with both DM (dashed lines) and E-MORB (continuous lines) compositions are after Aldanmaz *et al.* (2000). Short lines on each melting curve correspond to degrees of partial melting for a given mantle source. The Early Carboniferous basaltic samples tend to display higher degrees of melting (15–20%) than those responsible for the Late Carboniferous basaltic trachy-andesite (7–10%). (b) Yb v. La/Yb plot showing samples of Early Carboniferous basalts and Late Carboniferous trachy-andesite in the southwestern Tianshan Mountains. Also shown are model results for non-modal partial melting of garnet and spinel lherzolite sources containing different proportions of these minerals (100% garnet:0% spinel, 50%:50%, 20%:80% and 0%:100%) following the method of Class *et al.* (1994). The source is assumed to be enriched relative to chondritic composition (La = 1.79 ppm, Yb = 0.31 ppm). The model of garnet lherzolite is taken as Ol:Opx:Cpx:Grt = 60:25:9:6 and that of the spinel lherzolite as Ol:Opx:Cpx:Sp = 58:30:10:2. Phase proportions entering the melt are taken as Ol:Opx:Cpx:Grt (or Sp) = 10:20:65:5. Partition coefficients for La and Yb were selected from literature values (Lühr *et al.* 1995) as 0.0002:0.002:0.069:0.01:0.002 and 0.0015:0.049:0.28:4.1:0.007, for Ol:Opx:Cpx:Grt:Sp.

Conclusions

The Late Palaeozoic volcanic rocks with geochemical characteristics of arc magma, mainly consisting of basalt, trachyte, trachy-andesite, andesite and rhyolite, widely distributed in the southwestern Tianshan Mountains, represent the continental arc formed during the subduction of the Palaeo-southern Tianshan Ocean northwards under the Yili terrane. The zircon dating results demonstrate that this continental arc formed in the Late Devonian (>361 Ma, western part of the southwestern Tianshan Mountains) and Early Carboniferous (355–352 Ma, central part of the southwestern Tianshan Mountains) and was active until the Late Carboniferous in the eastern part of the southwestern Tianshan Mountains (c. 313 Ma). The studied volcanic rocks formed a volcanic chain greater than 600 km long. During the long history of arc evolution, the melt or fluid derived from Proterozoic gneissic biotite granite and/or sedimentary rocks in the subduction zone reacted with the mantle wedge. Consequently, the Proterozoic–Early Palaeozoic continental crust contributed to the Late Palaeozoic magma, as evidenced by the old inherited zircons with negative ϵ_{Hf} values as well as the negative ϵ_{Nd} values for the Late Devonian basaltic rocks. Calculation shows that the Late Devonian volcanic rocks formed by an AFC process between MORB and Proterozoic gneissic biotite granite, whereas the Carboniferous basaltic rocks originated by the partial melting of 8–20% lherzolite (the mantle wedge) with crustal contamination occurring locally and heterogeneously, as evidenced by the highly variable Sr–Nd–Hf isotopic compositions of the Late Carboniferous zircons.

M. Horstwood (British Geological Survey), M. Whitehouse and an anonymous reviewer provided detailed suggestions and critical comments, which helped us to improve this paper greatly. We also would like to express our gratitude to G. Zellmer, M. Elburg, Y. Zhang and Y. Zeng, who read through the early version of this paper. L. Xie and J. Yang helped us during isotope analysis. These and the financial support from NSFC (Grants 40730314, 40572033 and 40821002) are greatly appreciated.

References

- ALDANMAZ, E., PEARCE, J.A., THIRLWALL, M.F. & MITCHELL, J.G. 2000. Petrogenetic evolution of late Cenozoic, post-collision volcanism in western Anatolia, Turkey. *Journal of Volcanology and Geothermal Research*, **102**, 67–95.
- AN, F. & ZHU, Y.F. 2008. Study on trace elements geochemistry and SHRIMP chronology of volcanic rocks in Tulasu basin, northwest Tianshan. *Acta Petrologica Sinica*, **12**, 2741–2748 [in Chinese with English abstract].
- BALCAEN, L., SCHRUIVER, I.D., MOENS, L. & VANHAECKE, F. 2005. Determination of the $^{87}\text{Sr}/^{86}\text{Sr}$ isotope ratio in USGS silicate reference materials by multi-collector ICP–mass spectrometry. *International Journal of Mass Spectrometry*, **242**, 251–255.
- CHE, Z.C., LIU, L. & LIU, H.F. 1996. Review on the Ancient Yili rift, Xinjiang, China. *Acta Petrologica Sinica*, **12**, 478–490 [in Chinese with English abstract].
- CHEN, C., LU, H.F., JIANG, D., CAI, D.S. & WU, S.M. 1999. Closing history of the Tianshan oceanic basin, western China: an oblique collisional orogeny. *Tectonophysics*, **302**, 23–40.
- CHEN, J.F., MEN, F.S. & NI, S.B. 1995. Neodymium and strontium isotopic geochemistry of mafic–ultramafic intrusions from Qimulake rock belt, west Tianshan mountain, Xinjiang. *Geochemica*, **24**, 121–127 [in Chinese with English abstract].
- CHEN, Y.B., HU, A.Q., ZHANG, G.X. & ZHANG, Q.F. 2000. Precambrian basement age and characteristics of southwestern Tianshan: zircon U–Pb geochronology and Nd–Sr isotopic compositions. *Acta Petrologica Sinica*, **16**, 91–98 [in Chinese with English abstract].
- CLASS, C.R., ALTHERR, F., VOLKER, G., EBERZ, G. & MCCULLOCH, M.T. 1994. Geochemistry of Pliocene to Quaternary alkali basalts from the Huri Hills, northern Kenya. *Chemical Geology*, **113**, 1–22.
- COFFIN, M. & ELDHOLM, O. 1994. Large igneous provinces: crustal structure, dimensions, and external consequences. *Reviews of Geophysics*, **32**, 1–36.
- DEPAOLO, D.J. 1981. Trace elements and isotopic effects of combined wallrock assimilation and fractional crystallization. *Earth and Planetary Science Letters*, **53**, 189–202.
- GAO, J., LI, M.S., HE, G.Q., XIAO, X.C. & TANG, Y.Q. 1998. Paleozoic tectonic evolution of the Tianshan Orogen, northwestern China. *Tectonophysics*, **287**, 213–231.
- GOOLAERTS, A., MATTIELLI, N., DE JONG, J., WEIS, D. & SCOATES, J.S. 2004. Hf and Lu isotopic reference values for the zircon standard 91500 by MC-ICP-MS. *Chemical Geology*, **206**, 1–9.
- GREEN, N.L. 2006. Influence of slab thermal structure on basalt source regions and melting conditions: REE and HFSE constraints from the Garibaldi volcanic belt, northern Cascadia subduction system. *Lithos*, **87**, 23–49.
- HART, S.R. 1988. Heterogeneous mantle domains: signatures, genesis and mixing chronologies. *Earth and Planetary Science Letters*, **90**, 273–296.
- IZUKA, T. & HIRATA, T. 2005. Improvements of precision and accuracy in *in situ* Hf isotope microanalysis of zircon using the laser ablation-MC-ICPMS technique. *Chemical Geology*, **220**, 121–137.
- IMAI, N., TERASHIMA, S., ITOH, S. & ANDO, A. 1995. 1994 compilation values for GJ reference samples, 'Igneous rock series'. *Geochemical Journal*, **29**, 91–95.
- KURCHAVOV, A.M., GRANKIN, M.S., MALCHENKO, E.G., KHAMZIN, B.S. & ZHUKOVSKII, VI. 2002. Metallogenic zonality of the Devonian volcanoplutonic belt in Central Kazakhstan. *Geology of Ore Deposits*, **44**, 18–25 [in Russian].
- LUHR, J.F., ARANDA-GOMEZ, J.J. & HOUSH, T.B. 1995. San Quintin volcanic field, Baja California Norte, Mexico: geology, petrology, and geochemistry. *Journal of Geophysical Research*, **100**, 10353–10380.
- MAKSUMOVA, R.A., DZHENCHURAEVA, A.V. & BEREZANSKII, A.V. 2001. Structure and evolution of the Tien Shan Nappe–folded orogen. *Geologiya I Geofizika*, **42**, 1444–1452 [in Russian with English abstract].
- McKENZIE, D. & O'NIONS, R.K. 1991. Partial melt distribution from inversion of rare earth element concentrations. *Journal of Petrology*, **32**, 1021–1091.
- MOROZOV, YU. A. & TALITSKII, V.G. 2006. The Kyrgyz–Ata synform in the south Tien Shan: structural and kinematic aspects of its evolution. *Geotectonics*, **40**, 37–52.
- QIAN, Q., GAO, J., XIONG, X., LONG, L. & HUANG, D. 2006. Petrogenesis and tectonic settings of Carboniferous volcanic rocks from north Zhaosu, western Tianshan Mountains: constraints from petrology and geochemistry. *Acta Petrologica Sinica*, **22**, 1307–1323 [in Chinese with English abstract].
- PICKERING, K.T., KOREN, T.N., LYTOCHKIN, V.N. & SIVETER, D.J. 2008. Silurian–Devonian active-margin deep-marine systems and palaeogeography, Alai Range, Southern Tien Shan, Central Asia. *Journal of the Geological Society, London*, **165**, 189–210.
- ROLLINSON, H. 1993. *Using Geochemical Data: Evolution, Presentation, Interpretation*. Longman, New York.
- SHI, Y.S., LU, H.F., JIA, D. & HOWELL, D.G. 1994. Paleozoic plate tectonic evolution of the Tarim and western Tianshan Regions, Western China. *International Geological Review*, **36**, 1058–1066.
- SUN, S.S. & McDONOUGH, W.F. 1989. Chemical and isotope systematics of oceanic basalts: implications for mantle composition and processes. In: SAUNDERS, A.D. & NORRIS, M.J. (eds) *Magmaism in the Ocean Basins*. Geological Society, London, Special Publications, **42**, 313–345.
- UPADHYAY, D., SCHERER, E.E. & MEZGER, K. 2008. Fractionation and mixing of Nd isotopes during thermal ionization mass spectrometry: implications for high precision $^{142}\text{Nd}/^{144}\text{Nd}$ analyses. *Journal of Analytical Atomic Spectrometry*, **23**, 561–568, doi:10.1039/b715585a.
- VOLKOVA, N.I. & BUDANOV, V.I. 1999. Geochemical discrimination of metabasaltic rocks of the Fan–Karategin transitional blueschist/greenschist belt, South Tianshan, Tajikistan: seamount volcanism and accretionary tectonics. *Lithos*, **47**, 201–216.
- WANG, B.Y., LIANG, Z.J. & LI, X.D. 1994. *Comprehensive survey of geological sections in the west Tianshan of Xinjiang, China*. Science Publishing House, Beijing [in Chinese with English abstract].
- WANG, B., SHU, L.S., CLUZEL, D., FAURE, M. & CHARVET, J. 2007. Geochemical constraints on Carboniferous volcanic rocks of the Yili Block (Xinjiang, NW China): Implication for the tectonic evolution of Western Tianshan. *Journal of Asian Earth Sciences*, **29**, 148–159.
- WANG, C., LIU, L., LUO, J.H., CHE, Z.C., TENG, Z.H., CAO, X.D. & ZHANG, J.Y. 2007. Late Paleozoic post-collisional magmatism in the Southwestern Tianshan orogenic belt, take the Baleigong pluton in the Kokshal region as an example. *Acta Petrologica Sinica*, **23**, 1852–1872 [in Chinese with English abstract].
- WILLIAMS, I.S. 1998. U–Th–Pb geochronology by ion microprobe. In: MCKIBBEN, M.A., SHANKS, W.C., III & RIDLEY, W.I. (eds) *Applications of Microanalytical Techniques to Understanding Mineralization Processes*. Reviews in Economic Geology, **7**, 1–35.
- WINDLEY, B.F., ALLEN, M.B., ZHANG, C., ZHAO, Z.Y. & WANG, G.R. 1990.

- Paleozoic accretion and Cenozoic redeformation of the Chinese Tien Shan Range, central Asia. *Geology*, **18**, 128–131.
- WOODHEAD, J., HERGT, J. & SHELLEY, M. 2004. Zircon Hf-isotope analysis with an excimer laser, depth profiling, ablation of complex geometries, and concomitant age estimation. *Chemical Geology*, **209**, 121–135.
- WU, F.Y., YANG, Y.H., XIE, L., YANG, J.H. & XU, P. 2006. Hf isotopic compositions of the standard zircons and baddeleyites used in U–Pb geochronology. *Chemical Geology*, **234**, 105–126.
- XIA, L.Q., XIA, Z.C., XU, X.Y., LI, X.M., MA, Z.P. & WANG, L.S. 2004. Carboniferous Tianshan igneous megaprovince and mantle plume. *Geological Bulletin of China*, **23**, 903–910 [in Chinese with English abstract].
- XIAO, W.J., HANG, C.M., YUAN, C., ET AL. 2006. Unique Carboniferous–Permian tectonic–metalogenic framework of northern Xinjiang (NW China): constraints for the tectonics of the southern Paleosian Domain. *Acta Petrologica Sinica*, **22**, 1062–1076 [in Chinese with English abstract].
- XIE, X., YAN, M. & WANG, C. 1989. Geochemical standard reference samples, GSD 9-12, GSS 1-8 and GSR 1-6. *Geostandards Newsletter*, **13**, 125–133.
- XUE, Y.X. & ZHU, Y.F. 2009. Zircon SHRIMP chronology and geochemistry of the Haladala gabbro in south-western Tianshan Mts. *Acta Petrologica Sinica*, **25**, 1353–1363.
- XU, Y.G., CHUNG, S.L. & JAHN, B.M. 2001. Petrological and geochemical constraints on the petrogenesis of the Permo-Triassic Emeishan flood basalts in southwestern China. *Lithos*, **58**, 145–168.
- YANG, J.H., WU, F.Y., CHUNG, S.L., WILDE, S.A. & CHU, M.F. 2006. A hybrid origin for the Qianshan A-type granite, northeast China: Geochemical and Sr–Nd–Hf isotopic evidence. *Lithos*, **89**, 89–106.
- ZHANG, L.F., ELLIS, D.J., ARCULUS, R.J., JIANG, W.B. & WEI, C.J. 2003. Ultra-deep subduction of carbonates to the mantle: evidence from the carbonate reaction of magnesite + calcite (aragonite) = dolomite in metapelites from western Tianshan, China. *Journal of Metamorphic Geology*, **21**, 523–529.
- ZHANG, L.F., AI, Y.L., LI, X., RUBATTO, D. & SONG, B. 2007. Triassic collision of western Tianshan orogenic belt, China: Evidence from SHRIMP U–Pb dating of zircon from HP/UHP eclogitic rocks. *Lithos*, **96**, 266–280.
- ZHAI, W., GAO, J. & SUN, X. 2006. The wallrocks of the Axi gold deposit—Dahalajunshan Group: its zircon SHRIMP dating. *Acta Petrologica Sinica*, **22**, 1399–1406 [in Chinese with English abstract].
- ZHAO, Z.H., XIONG, X.L., WANG, Q., BAI, Z.H., XU, J.F. & QIAO, Y.L. 2004. Association of Late Paleozoic adakitic rocks and shoshonitic volcanic rocks in the western Tianshan, China. *Acta Geologica Sinica (English Edition)*, **78**, 68–72.
- ZHAO, Z.H., WANG, Q., XIONG, X.L., NIU, H.C., ZHANG, H.X. & QIAO, Y.L. 2007. Magnesian igneous rocks in northern Xinjiang. *Acta Petrologica Sinica*, **23**, 1696–1707 [in Chinese with English abstract].
- ZHU, Y.F., ZHANG, L.F., GU, L., GUO, X. & ZHOU, J. 2005. The zircon SHRIMP chronology and trace element geochemistry of the Carboniferous volcanic rocks in western Tianshan Mountains. *Chinese Science Bulletin*, **50**, 2201–2212.
- ZHU, Y.F., ZHOU, J., SONG, B., ZHANG, L.F. & GUO, X. 2006a. Age of the ‘Dahalajunshan’ formation in Xinjiang and its disintegration. *Geology in China*, **33**, 487–497 [in Chinese with English abstract].
- ZHU, Y.F., GUO, X. & ZHOU, J. 2006b. Petrology and geochemistry of a ^{+8}Nd gabbro body in Baluntai region, central Tianshan mountains, Xinjiang. *Acta Petrologica Sinica*, **22**, 1178–1192 [in Chinese with English abstract].

Received 27 October 2008; revised typescript accepted 14 July 2009.

Scientific editing by Martin Whitehouse.